

SLCs contribute to endocrine resistance in breast cancer: role of SLC7A5 (LAT1)

Authors: Catherine M. Seigny¹, Surojeet Sengupta¹, Zhexun Luo¹, Xiaoyi Liu¹, Rong Hu¹, Zhen Zhang², Lu Jin¹, Dominic Pearce³, Diane Demas¹, Ayesha N. Shajahan-Haq¹, and Robert Clarke¹

Addresses: 1) Department of Oncology, Georgetown University, Washington, DC 20057. 2) Department of Pathology, Johns Hopkins Medical Institutions, Baltimore, MD 21231, USA Johns Hopkins University. 3) Applied Bioinformatics of Cancer, University of Edinburgh Cancer Research UK Centre, MRC Institute of Genetics and Molecular Medicine, Edinburgh, UK

Short Title: LAT1 in Endocrine Resistance

Keywords: SLC7A5 (LAT1), Endocrine Therapy Resistance, Breast Cancer

Corresponding Author: Catherine M. Seigny cs1507@georgetown.edu

Abstract:

Resistance to endocrine therapies remains a major challenge for the successful management of patients with estrogen receptor-positive (ER+) breast cancers. Central to the development of resistance is the adaptive reprogramming of cellular metabolism in response to treatment. Solute carriers (SLCs) play a key role in metabolic reprogramming by transporting sugars, amino acids, and other nutrients and regulating their abundance within the cell and its subcellular organelles. We found 109 SLC mRNAs to be differentially expressed between endocrine sensitive and resistant breast cancer cells. In univariate analyses, 55 of these SLCs were associated with poor outcome in ER+ breast cancer patients. Data from TMT and SILAC studies then led us to focus on SLC7A5 (LAT1). In complex with SLC3A2 (CD98), LAT1 is the primary transporter of large, neutral amino acids including leucine and tyrosine. LAT1 expression is estrogen-regulated in endocrine sensitive cells but this regulation is lost in resistant cells. Pharmacologic inhibition or genetic depletion of LAT1 each suppressed growth in two models of endocrine resistant breast cancer. Autophagy was activated with LAT1 inhibition, but cells failed to degrade p62 showing that flux was blocked. Overexpression of the LAT1 cDNA increased protein synthesis and high LAT1 expression correlated with poor disease-free survival in ER+ breast cancer patients. This study uncovers a novel LAT1 mediated adaptive response that contributes to the development of endocrine resistance. Blocking LAT1 function may offer a new avenue for effective therapeutic intervention against endocrine resistant ER+ breast cancers.

Introduction:

In the United States, breast cancer is the most commonly diagnosed cancer in women¹. Of the 253,000 newly diagnosed breast cancers each year, approximately 70% are estrogen receptor positive (ER+)². Endocrine therapies, such as aromatase inhibitors (AIs) and selective estrogen receptor modulators (SERMs), have extended life expectancy for patients with ER+ disease³. Unfortunately, resistance to these treatments is common^{4,5}. Patients who do not initially respond to endocrine therapies (*de novo* resistance), or who initially respond but eventually recur (acquired resistance), generally require cytotoxic chemotherapies. Chemotherapy often induces serious side effects⁶ but is rarely curative in advanced disease. It is critical to understand how resistance to endocrine therapy develops and to design more effective treatments for patients. Ideally, this can be achieved while minimizing toxicity.

Dysregulation of cellular energetics, a key hallmark of cancer, is driven by altered metabolism in cancer cells compared with normal cells^{7,8}. Unique aspects of cancer cell metabolism can use pro-survival mechanisms, such as autophagy, to survive under stress or in a nutrient-poor microenvironment. Autophagy is an intracellular process of lysosomal degradation of proteins and organelles that can release amino acids, sugars, and other essential nutrients to support cell metabolism^{9,10} and help to meet cellular energy demand¹¹. If proliferation does not resume and autophagy remains active at a high level, autophagy can switch from being pro-survival to activating cell death. Previously, we have shown that endocrine resistant cells exhibit a higher autophagy efficiency than sensitive cells¹². Differential expression of proteins involved in metabolism

likely contributes to maintaining the balance between pro-survival autophagy and pro-apoptotic responses to endocrine therapies¹³.

We used established models of endocrine resistant breast cancer to assess changes in the patterns of protein expression of sensitive (LCC1¹⁴; estrogen independent, tamoxifen sensitive) and resistant (LCC9¹⁵; estrogen independent, tamoxifen and fulvestrant cross resistant) cells¹⁵. We also used the T47D variants T47D:A18 (estrogen dependent, tamoxifen sensitive), T47D:A18-4HT¹⁶ (estrogen independent, tamoxifen resistant) and T47D:C42¹⁷ (estrogen receptor negative, tamoxifen resistant). Together, these models reflect the endocrine therapy sensitive and resistant phenotypes that exist in some patient cohorts. Differential mRNA expression analysis of endocrine sensitive (LCC1) and endocrine resistant (LCC9) cells implicated several solute carriers (SLCs) in acquired endocrine resistance. At the mRNA level, we found altered expression of 109 members of the SLC gene family; 16 of these genes were confirmed to be differentially expressed by unbiased proteome analyses. Two quantitative proteomic approaches were used to study differential protein expression of LCC1 and LCC9 cells: 1) tandem mass tag (TMT) and 2) stable isotope labeling with amino acids in cell culture (SILAC). We hypothesized that changes in solute carriers (SLCs) expression and nutrient uptake may supplement autophagy to support the cellular metabolism that drives an endocrine resistant phenotype.

SLCs are transport proteins that can act as exchangers, cotransporters, facilitated transporters, or orphan transporters for key nutrients such as amino acids or sugars¹⁸. Here we show that the solute carrier family 7 (SLC7) has several members upregulated in resistant compared with sensitive cells. SLC7s transport amino acids into cells and can

feed intermediate metabolism^{12,19}. Amino acids can be modified to enter the citric acid cycle, such as with the conversion of leucine into acetoacetate^{20,21}. SLC7A5 (also known as LAT1) and/or its interacting partner SLC3A2 (CD98) is upregulated in a variety of cancers^{22–26} and is critical for growth and survival. Amino acids including the essential amino acid leucine and the non-essential amino acid tyrosine are transported into the cell through LAT1^{23,27}. For example, upregulation of LAT1 during androgen therapy can drive pancreatic cancer progression²², whereas homozygous knockout of LAT1 is embryonic lethal in mice²⁸. We chose to focus here on LAT1 because it was significantly upregulated in the LCC9 compared to the LCC1 cells in both proteome analyses and in the transcriptome analysis. We now establish a critical role for LAT1 overexpression in enabling the growth of endocrine resistant breast cancer cells.

Materials and Methods:

Cell lines: LCC1²⁹ cells (antiestrogen sensitive) and LCC9¹⁵ cells (antiestrogen resistant) were obtained from stocks maintained by the Georgetown Tissue Culture Shared Resource. LCC1 and LCC9 cells were cultured in 5% charcoal stripped calf serum (CCS) in phenol red free modified IMEM media (Life Technologies). The MCF7:WS8 cells and T47D cell variants were a gift from Dr. V.C. Jordan at MD Anderson. MCF7:WS8³⁰ cells were maintained in 5% fetal bovine serum in modified IMEM media (Life Technologies). T47D:A18 cells and T47D:A18-4HT¹⁶ cells were grown in 5% fetal bovine serum (FBS) in RPMI (Life Technologies). T47D:C42¹⁷ cells were grown in 5% charcoal stripped calf serum in phenol red free modified RPMI media (Life Technologies). These cells represent acquired estrogen independence and endocrine therapy resistance in estrogen receptor positive breast cancer. All cells grown in FBS media were estrogen deprived in CCS media for 72 hours before experimental use. All experiments were done in triplicate unless stated otherwise.

Stable isotope labelling by amino acids in cell culture (SILAC): MCF7:LCC1 and MCF7:LCC9 cells were double-labelled in presence of heavy (C13) or light (C12) arginine and lysine amino acids. The cells were cultured for at least five doublings before being harvested and snap frozen. Replicates were collected using the label switch approach to assess robustness. MS Bioworks, (Ann Arbor, MI, USA) carried out the SILAC experiments. Label incorporation of more than 98% was confirmed for both the cell lines. The samples were washed with PBS and lysed with RIPA. Ten microgram total protein of light and heavy labelled samples were combined and the combined samples were processed by SDS-PAGE. For each sample, the mobility region was excised into 20 equal

sized segments. Each segment was processed by in-gel digestion. Each gel digest was analyzed by nano LC-MS/MS with a Waters NanoAcquity HPLC system interfaced to a ThermoFisher Q Exactive mass spectrometer. Data were processed using MaxQuant version 1.5.3.17 (Max Planck Institute for Biochemistry) that incorporates the Andromeda search engine.

Pharmacological agents: 17 β -estradiol (Cat# E-8875) was purchased from Millipore Sigma (MA, USA). 4-hydroxytamoxifen (Cat# 3412) and fulvestrant (Cat# 1047) were purchased from Tocris (Bristol, United Kingdom) and used at pharmacologically relevant concentrations^{15,31}. JPH203 (Cat# 406760) was purchased from MedKoo Biosciences Inc. (NC, USA).

Plasmids and transfections: SLC7A5 siRNA and plasmid DNA were obtained from OriGene. Products used were SLC7A5 (ID 8140) Trilencer-27 Human siRNA and SLC7A5 (NM_003486) Human cDNA ORF Clone. GRP78 (HSP5A) siRNA was purchased from Dharmacon (L-008198-00-0005). Transfections for siRNA used Invitrogen's Lipofectamine RNAiMAX and for plasmid DNA we used Lipofectamine LTX Plus (ThermoFisher, MA, USA). Cells were treated for 24 hours then refed with fresh growth medium for another 48 hours before collection for protein or growth assay in knockdown experiments. For overexpression experiments, cells were transfected with the appropriate cDNA construct for 4 hours in serum free media before the media was changed to 5% CCS IMEM for an additional 44 hours.

Crystal violet cell assay: To measure changes in cell growth, 10,000-15,000 cells were plated into each well of a 24-well plate. Treatments were started after 24 hours of seeding (Day 0) and the initial plate was collected as the baseline measurement. At the time of

harvest, cells were washed with 1X PBS and rocked in 200 μ L crystal violet solution (2.5 g crystal violet, 125 mL methanol, 375 mL water) for 30 minutes. Plates were rinsed in deionized water and allowed to air-dry for 48 hours. Once all time points were collected, citrate buffer was used to extract dye. Analysis of the intensity of staining, which directly reflects cell number, was then assessed at 570 nm using a VMax kinetic microplate reader (Molecular Devices Corp., Menlo Park, CA)^{13,32}.

Western blotting: Total protein was collected in radioimmunoprecipitation buffer (RIPA) with PhosSTOP (Roche Diagnostics, Mannheim, Germany) and Complete Mini protease inhibitor cocktail tablets (EMD Chemicals Inc. San Diego, CA). Quantification was done using Pierce BCA protein assay (Thermo Fischer Scientific) and 20 μ g were separated by NuPAGE 4-12% Bis-Tris gel (Invitrogen). Primary antibodies used were LAT1 (Cat #5347S, 1:1,000; Cell Signaling), CD98 (Cat# sc-376815, 1:1,000; Santa Cruz), ER alpha (Cat# sc-543, 1:1,000; Santa Cruz Biotechnology), and β -Actin (Cat# 66009-1-Ig, 1:10,000; Protein Tech). Secondary antibodies used were Anti-rabbit IgG, HRP-linked Antibody #7074 (1:2,000; Cell Signaling) and Anti-mouse IgG, HRP-linked Antibody #7076 (1:2,000; Cell Signaling).

RNA isolation and qRT-PCR: RNA was isolated using the trizol reagent (Invitrogen, CA, USA) and Qiagen RNeasy mini kit (CA, USA) according to the manufacturer's instructions. 1 mL of trizol was used per well of a 6-well plate, mixed with 200 μ L of chloroform, and incubated at room temperature for 15 minutes. The solution was spun at 15,000 rpm for 15 minutes and the top aqueous layer removed and mixed with an equal volume of 70% ethanol before loading onto the column of the RNeasy kit and processed as described by the manufacturer. Quantification was done using a nano-drop ND-1000

Spectrophotometer. cDNA was made using High Capacity cDNA Reverse Transcription Kit (Thermo Fischer Scientific) to prepare cDNA from 1000 ng RNA. PowerUp SYBR Green Master Mix from Life Technologies was used for qRT-PCR. Primers used were IDT SLC7A5 (FW: CGA GGA GAA GGA AGA GGC G; RV: GTT GAG CAG CGT GAT GTT CC), SLC3A2 (FW: GTC GCT CAG ACT GAC TTG CT; RV: GTT CTC ACC CCG GTA GTT GG), and 36B4 (FW: GTG TTC AAT, GGC, AGC, AT; RV: GAC ACC CTC CAG GAA GCG A). Analysis of the data followed the delta-delta CT method³³.

Immunofluorescence staining: 10,000-50,000 cells were plated onto glass cover slips 24 hours before treatment. Immunofluorescence experiments were performed on cells after 24 hours of either vehicle or 1 nM 17 β -estradiol exposure. Cells were fixed with PBS containing 3.2% paraformaldehyde (Cat# 15714, PA, USA) with 0.2% Triton X-100 (Cat# T8532-500mL, SIGMA, MA, USA) for 5 minutes before being washed with PBS. Cells were incubated in methanol in the -20 °C for 20 minutes. Cells were washed again before being exposed to primary antibody in the presence of an antibody block containing 10% goat serum. Primary antibodies were as described in the western blotting protocol above; the concentration of LAT1 was 1:100 and was 1:50 for CD98. Secondary antibodies used were Alexa Fluor 594 anti-rabbit (Cat# A-11012, Life Technologies) and Alexa Fluor 488, anti-mouse (Cat # A-11001, Life Technologies).

Cell cycle analysis: Cells were fixed in 75% ethanol and analyzed by FACS analysis (Georgetown Flow Cytometry/Cell Sorting Shared Resource). Cell sorting of GFP-positive cells was done in 5% CCS Media by the Georgetown Flow Cytometry/Cell Sorting Shared Resource then collected for protein or analyzed for cell cycle analysis. Data were acquired

using flow cytometry (BD LSRFortessa; BD Biosciences) and data analysis was performed using FCS express 6 software (De Novo Software, Glendale, CA)

Clinical correlation analyses: We studied only data from invasive ER+ breast cancers that received at least one endocrine therapy (tamoxifen) from the following publicly available datasets (GSE2990³⁴, GSE6532-a³⁵, GSE6532-p³⁵, GSE9195³⁶). Data were analyzed as described by Pearce *et al*³⁷. For each probe of interest, the dataset was sorted by the normalized expression value in ascending order. Within each sorted sub-dataset, a cursor was set to move up one sample per iteration through the entire dataset starting from the sample with smallest expression value. At each iteration, survival analysis was performed by comparing the samples on either side of the cursor. The resulting statistics including hazard ratio and log rank test p-value provided one measure of significance per possible division in a dataset. In this study, we used 4 independent clinical datasets and 119 genes (probeset_ids). An additional unpublished dataset (GSE46222) was also analyzed and the results are shown in Table 1.

Statistical Analysis: ANOVA was used to determine significance (SigmaPlot) with a Dunnett's *post hoc* test applied when multiple comparisons were made to a common control.

Results

From microarray analysis of LCC1 and LCC9 mRNA we identified 109 differentially regulated solute carriers (SLCs)^{38,39}. Of those 109 solute carriers (SLCs), 55 were associated with poor clinical outcome (Table 1). When mapped onto the proteomic data (TMT and SILAC), three SLCs: SLC2A1, SLC3A2, and SLC7A5 (Table 2) were each upregulated at least 1.5 fold. We had previously studied SLC2A1 (GLUT1) and found that glucose and glutamine uptake are regulated by MYC¹³. Here, we have focused on SLC7A5 (LAT1) and its protein partner SLC3A2 (CD98) to determine their role in endocrine therapy resistance.

LAT1 is regulated by estrogen and upregulated in endocrine therapy sensitive cells:

We used MCF7, LCC1, LCC9,¹⁵ T47D:A18, T47D:C42, and T47D:4HT¹⁷ cells as models to study the role of LAT1 in endocrine resistance. From the three analyses, we found that LAT1 was significantly upregulated in the endocrine resistant LCC9 compared with endocrine sensitive LCC1 cells. Previously, LAT1 (SLC7A5) mRNA has been reported to be induced by estrogen in MCF7 cells⁴⁰. We confirmed this observation for LAT1 protein in MCF7 cells (Figure 1A) and found a similar induction in LCC1 and T47D:A18 cells (Figure 1A&B). Endocrine resistant LCC9, T47D:4HT, and T47D:C42 cells expressed significantly higher basal levels of total LAT1 protein than their respective (sensitive) parental cell lines. Since these data infer estrogen regulation of LAT1 by the estrogen receptor (ER; ESR1), we used ENCODE to analyze ChIA-PET data from MCF7 cells^{41,42}. Using the integrative genomics viewer, we found an ER-occupied site on the LAT1 gene (Figure 1C; Supplemental Figure 1 for whole gene)⁴³.

Endocrine sensitive cells doubled their LAT1 protein expression when treated with estrogen for 24 hours. The LAT1 mRNA and protein expression increased in response to estrogen over time in both MCF7 and LCC1 cells (Figure 1D-F). After 12 to 24 hours of estrogen treatment, LAT1 mRNA levels were significantly upregulated ($p < 0.05$). In contrast to the endocrine sensitive models, LCC9 and T47D:C42 cells both showed an increase in basal LAT1 protein expression but no further increase of LAT1 was seen after 24 hours of estrogen treatment.

E2 regulation of LAT1 is lost in endocrine resistant LCC9 cells:

Since we observed an estrogen-induced increase of LAT1 protein and mRNA expression in sensitive cell lines, we next studied an extended estrogen time course treatment in resistant cells. Levels of LAT1 mRNA and protein did not change in response to estrogen with increased time of treatment in the resistant LCC9 cells (Figure 2A-B). This loss of regulation did not affect either basal expression levels or membrane subcellular co-localization of the LAT1 and CD98 proteins. Protein co-localization was measured in immunofluorescence experiments where both MCF7 and LCC9 cells were treated with either vehicle or estrogen (Figure 2C-D respectively).

LAT1 is differentially expressed in response to endocrine therapy treatment:

To determine the effect of endocrine therapies on LAT1 expression, combinations of estrogen and either tamoxifen or fulvestrant were used to determine how LAT1 was regulated in response to estrogen treatment. MCF7 (Figure 3A), LCC1 (Figure 3B), and LCC9 cells (Figure 3C) express both mRNA and protein for LAT1 and CD98. LAT1 expression was significantly increased in response to estrogen or tamoxifen in the sensitive models but unchanged in resistant models. Fulvestrant decreased LAT1

expression in MCF7 and LCC1 cells treated with E2 or tamoxifen, suggesting that ER inhibition negatively affects LAT1 expression. Estrogen alone, tamoxifen alone, and estrogen and tamoxifen cotreatment each significantly increased LAT1 mRNA ($p < 0.05$) in both sensitive models. In the MCF7 cells, addition of fulvestrant with tamoxifen did not return LAT1 mRNA levels fully to baseline (upregulation $p < 0.05$). In the MCF7 models the classical estrogen-regulated GREB1 mRNA was not upregulated in response to tamoxifen but increased in response to estrogen (Supplemental Figure 2A-B). GREB1 mRNA was unchanged in the LCC9 cells in response to endocrine treatments (Supplemental Figure 2C). In the T47D models, the same trend was seen between the endocrine sensitive T47D:A18s and resistant T47D:C42 and T47D:4HT cells (Supplemental Figure 3).

LAT1 inhibition restricts cell growth and induces G1 arrest

Since LAT1 had increased basal expression and lost estrogenic regulation in resistant cells, we targeted LAT1 function using JPH203, a tyrosine analog and selective inhibitor of LAT1 function^{44,45}. We applied a time- (3 to 6 days) and dose-dependent study design (12.5 - 50 μ M) to determine how MCF7 and LCC9 cells respond to JPH203 treatment (Figure 4A-B). Growth was significantly inhibited by ~50% with 50 μ M JPH203 in both cell lines in the presence or absence of estrogen ($p > 0.05$). The effect of JPH203 treatment increased when we reduced the concentration of essential amino acids in the media in a dose-dependent manner (Supplemental Figure 4). We also used two individual siRNAs to knock-down LAT1 expression. 72 hours after transfection, LAT1 protein expression was decreased by 40-60% as confirmed by Western blot hybridization (Figure 4C-D). Cell growth was significantly decreased with two individual siRNAs targeting LAT1 (Figure 4E,

p<0.05) after 3 or 6 days compared with control. To determine how LAT1 inhibition affected cell cycle distribution, we performed cell cycle analysis of MCF7 and LCC9 cells treated with either 50 μ M JPH203 or with siLAT1. While JPH203 inhibition did not change cell cycle phase distribution of the MCF7 or LCC9 cells, treatment with siLAT1 decreased the proportion of cells in S phase (Figures 4F-H). Puromycin is an inhibitor of global protein synthesis and can be used to assess translation by treating cells with a high dose followed by a western blot⁴⁶. LCC9 cells treated with siLAT1 followed by puromycin treatment exhibited a decrease in global protein translation (Figure 4I). Targeting LAT1 either pharmacologically or genetically was effective in reducing growth of the resistant cells.

Overexpression of LAT1 increases S phase and global protein translation

MCF7 and LCC1 cells were transfected with plasmids containing either a GFP-empty vector or GFP-LAT1 cDNA. Overexpression of LAT1 protein was confirmed in MCF7 and LCC1 cells by measuring protein expression (Figure 5A and 5B respectively). Fluorescence imaging of the GFP tag (Figure 5C) also confirmed plasmid expression. Puromycin treatment of transfected cells showed an increase in global protein translation (Figure 5D). In addition to increased global translation in the sensitive cells, we observed an increased trend for cells to be in S phase in both MCF7 and LCC1 cells (Figure 5E).

Autophagy increases with LAT1 inhibition

Increased autophagy is a feature of endocrine resistant cells^{12,47} that may cooperate with increased nutrient scavenging by SLCs to support the restoration of metabolic homeostasis. Autophagic flux can be estimated by measuring the expression of two key proteins: LC3 and p62⁴⁸. Apoptosis can be evaluated by western blot hybridization of the

cleavage of poly(ADP-ribosyl) polymerase (PARP)⁴⁹. Expression of both the LC3 and p62 proteins was increased following siRNA knockdown of LAT1 (Figure 5A). LC3 expression increased but p62 did not decrease. These data are consistent with an induction of autophagy but incomplete autophagic flux. Neither PARP cleavage nor phosphorylation of eIF2a was observed, suggesting that apoptosis and the PERK pathway within the unfolded protein response (UPR) are not required for this process. Knockdown of GRP78 in LCC9 cells (BiP; controls all three pathways within the UPR including PERK) produced a non-significant increase in LAT1 protein expression, whereas LAT1 mRNA expression was significantly increased (Figure 6C and D). These data imply either an increased rate of GRP78 protein turnover or a delay in increasing mRNA translation; determining the precise mechanism is beyond the scope of the current study.

Higher LAT1 expression correlates with poor clinical outcome

To determine the clinical relevance of LAT1 in endocrine-treated ER+ breast cancer, we established the association of LAT1 mRNA expression with clinical outcomes in four gene expression data sets (Figure 7, see Materials and Methods). We studied only invasive ER+ breast cancers that received at least one endocrine therapy. Data sets were analyzed as described by Pearce et al.³⁷ Higher LAT1 expression correlates with a poor disease-free survival (From KM plots GSE2290 $p=0.007$, GSE6532-a $p=0.005$, GSE6532-p $p=0.037$, GSE9195 $p=0.01$ and Table 2).

Discussion:

While tamoxifen and fulvestrant are effective endocrine therapies³, further research is needed to prevent or overcome the development of resistance. Endocrine therapy resistance, particularly in advanced disease, is a major clinical challenge for patients and their physicians. Matched sensitive and resistant cell lines are useful tools to study changes in cell processes as endocrine therapy resistance develops. By performing mRNA, TMT, and SILAC analyses of differentially regulated genes, we identified several key players associated with the development of acquired resistance (Table1). SLC7A5 (LAT1) was significantly upregulated in the LCC9 compared with the LCC1 cells in all three analysis. This observation led to our focus on LAT1 to determine its role in the development or maintenance of endocrine therapy resistance.

LAT1 has been proposed as a biomarker for progression in breast cancers⁵⁰. However, the role of LAT1 in the context of endocrine therapy responsiveness is unknown. Our study shows that LAT1 overexpression in endocrine resistant breast cancer cells contributes to their survival and growth. For example, we establish that LAT1 mRNA and protein expression are increased in endocrine resistant breast cancer cells compared with their genetically related but endocrine sensitive counterparts. LAT1 is reported to be estrogen regulated⁴⁰; we confirmed this observation using ER positive MCF7 and T47D breast cancer cells. Constitutive activation of the ER is one component of endocrine resistance that results in the dysregulation of a number of downstream genes⁵¹. Notably, in endocrine resistant cells the basal expression of LAT1 was higher and its estrogenic regulation was lost. A drug-induced reduction of amino acid uptake in sensitive cells could lead to metabolic stress and ultimately cell death. Resistant cells

must find a way to address this limitation. Upregulation of SLCs such as LAT1 could improve a cell's ability to scavenge nutrients from the tumor microenvironment, a function that is critical for cell survival⁵². LAT1 is responsible for the uptake of leucine and tyrosine for protein synthesis or as intermediates to enter the TCA cycle^{19,53,54}. Increased LAT1 expression has been reported in several cancers including prostate cancer²², pleural mesothelioma²⁴, multiple myeloma²⁵ and non-small cell lung cancer²⁶. Since homozygous knockout of LAT1 in embryonic lethal²⁸, LAT1 is critical for growth and survival.

While LAT1 is under estrogen regulation in MCF7 and LCC1 cells, this is lost in the resistant cells. LAT1 expression was increased by tamoxifen treatment in both MCF7 and LCC1 cells; this increase was reduced by fulvestrant. These observations are likely reflective of the partial agonist activity of tamoxifen and further imply that LAT1 expression is under estrogenic regulation. MYC is also under estrogenic regulation and we have shown that MYC can regulate glucose and glutamine through the unfolded protein response in endocrine resistant cells¹³. LAT1 upregulation in endocrine resistance may cooperate with MYC-induced increases in glucose and glutamine metabolism to contribute to cell survival in the face of the stress induced by endocrine therapies.

Targeting solute carriers has not been widely explored in breast cancer. JPH203 was less effective than a targeted siRNA knockdown to restrict cell growth and induce G1 arrest. However, free tyrosine, leucine, and phenylalanine in media likely influenced the efficacy of JPH203; these and other free amino acids also may be accessible within the tumor microenvironment. siRNA knock-down of LAT1 also initiated autophagy and decreased global protein translation in endocrine resistant LCC9 cells. The latter could be controlled by activation of the UPR⁵⁶, which can also regulate autophagy^{12,47}. Inhibiting

LAT1 would reduce amino acid uptake that could activate autophagy in an attempt to restore metabolic homeostasis. However, LAT1 inhibition lead to an initiation of autophagy but flux did not complete and cell death occurred. Knocking down GRP78, the primary regulator of the unfolded protein response (UPR)⁵⁷, increased LAT1 expression after 72 hours. It is likely that the uptake of amino acids and the ability of UPR to regulate global protein translation are connected, perhaps by activating features of the UPR.

JPH203 showed antineoplastic activity and safety for biliary tract and colorectal cancer in the Phase I clinical trial reported by Okana et. al.⁵⁸ While LAT1 inhibitors have not yet been tested in breast cancer patients, the drug appears to be well tolerated. Targeting LAT1 limits the amount of amino acids, particularly leucine and tyrosine, that can enter the TCA cycle or maintain the production of new proteins^{27,40}. Using JPH203 in combination with endocrine therapies and/or mTOR inhibitors⁵⁹ could prove beneficial. For example, the combination of JPH203 and mTOR inhibitors could result in decreased amino acid uptake and protein translation to restrict tumor cell growth. Further exploration into the metabolic fate of the increased uptake of pre-formed amino acids could provide useful insights into the metabolic adaptations required to maintain endocrine resistance. Imaging of leucine or tyrosine with positron emission tomography (PET)⁶⁰ could be clinically informative as a potential biomarker of endocrine responsiveness in ER+ breast tumors.

Finally, we show that LAT1 overexpression is consistently associated with poor relapse free survival in four independent clinical datasets from ER+ patients that received an endocrine therapy. This observation is consistent with other reports that LAT1 may be an indicator of poor prognosis^{25,61}. Taken together with the mechanistic outcomes

384 reported here, further study of LAT1 and its role in endocrine therapy resistance may lead
385 to novel therapeutic alternatives to improve overall survival for patients.

386

Acknowledgements

This work was supported by Public Health Service Awards U54-CA149147, U01-CA184902 (R Clarke) and Department of Defense Breast Program W81XWH-18-1-0722 (R Clarke) and Lombardi Comprehensive Cancer Center Support Grant (CCSG) NIH P30 CA051008. We thank Karen Creswell and Dan Xun for their help at the Flow Cytometry Shared Resource at Georgetown-Lombardi Comprehensive Cancer Center. The views and opinions of the author(s) do not reflect those of the US Army or the Department of Defense.

References:

1. Torre, L. A., Islami, F., Siegel, R. L. & Ward, E. M. CEBP FOCUS : Global Cancer in Women Global Cancer in Women : Burden and Trends. **26**, 444–458 (2017).
2. Siegel, R. L., Miller, K. D. & Jemal, A. Cancer statistics, 2017. *CA. Cancer J. Clin.* **67**, 7–30 (2017).
3. Burstein, H. J. *et al.* Adjuvant Endocrine Therapy for Women With Hormone Receptor–Positive Breast Cancer: ASCO Clinical Practice Guideline Focused Update. *J. Clin. Oncol.* JCO.18.01160 (2018). doi:10.1200/JCO.18.01160
4. Reinert, T. & Barrios, C. H. Optimal management of hormone receptor positive metastatic breast cancer in 2016. *Ther. Adv. Med. Oncol.* **7**, 304–320 (2015).
5. Ballinger, T. J., Meier, J. B. & Jansen, V. M. Current Landscape of Targeted Therapies for Hormone-Receptor Positive, HER2 Negative Metastatic Breast Cancer. *Front. Oncol.* **8**, 308 (2018).
6. Condorelli, R. & Vaz-Luis, I. Managing side effects in adjuvant endocrine therapy for breast cancer. *Expert Rev. Anticancer Ther.* **18**, 1101–1112 (2018).
7. Hanahan, D. & Weinberg, R. A. Hallmarks of cancer: The next generation. *Cell* **144**, 646–674 (2011).
8. De Berardinis, R. J. & Chandel, N. S. Fundamentals of cancer metabolism. *Sci. Adv.* **2**, (2016).
9. Rabinowitz, J. & White, E. Autophagy and Metabolism. *Acc. Chem. Res.* **45**, 788–802 (2008).
10. White, E., Mehnert, J. M. & Chan, C. S. Autophagy, Metabolism, and Cancer. **21**, 5037–5046 (2015).
11. Mathew, R., White, E., Athew, R. M. & Hite, E. W. Autophagy , Stress , and Cancer Metabolism : What Doesn ’ t Kill You Makes You Stronger Autophagy , Stress , and Cancer Metabolism : What Doesn ’ t Kill You Makes You Stronger. **LXXVI**, 389–396 (2012).
12. Cook, K. L. *et al.* Knockdown of estrogen receptor- α induces autophagy and inhibits antiestrogen-mediated unfolded protein response activation, promoting ROS-induced breast cancer cell death. *FASEB J.* **28**, 3891–905 (2014).
13. Shajahan-Haq, A. N. *et al.* MYC regulates the unfolded protein response and glucose and glutamine uptake in endocrine resistant breast cancer. *Mol. Cancer* **13**, 239 (2014).
14. Brunner, N., Fojo, A., Freter, C. E., Lippman, M. E. & Clarke, R. Acquisition of Hormone-independent Growth in MCF-7 Cells Is Accompanied by Increased Expression of Estrogen-regulated Genes but Without Detectable DNA Amplifications. *Cancer Res.* **53**, 283–290 (1993).
15. Brunner, N. *et al.* MCF7-LCC9 : An Antiestrogen-resistant MCF-7 Variant in Which Acquired Resistance to the Steroidal Antiestrogen ICI 182 , 780 Confers an Early Cross Resistance to the Nonsteroidal Antiestrogen Tamoxifen. (1997).

- 435 16. Murphy, C. S., Meisner, L. F., Wu, S. Q. & Jordan, V. C. Short- and long-term estrogen
436 deprivation of T47D human breast cancer cells in culture. *Eur. J. Cancer Clin. Oncol.* **25**,
437 1777–1788 (1989).
- 438 17. Pink, J. J., Bilimoria, M. M., Assikis, J. & Jordan, V. C. Irreversible loss of the oestrogen
439 receptor in T47D breast cancer cells following prolonged oestrogen deprivation
440 [published erratum appears in Br J Cancer 1997;75(10):1557]. *Br J Cancer* **74**, 1227–
441 1236 (1996).
- 442 18. Hediger, M. A. *et al.* The ABCs of solute carriers: Physiological, pathological and
443 therapeutic implications of human membrane transport proteins. *Pflügers Arch. Eur. J.*
444 *Physiol.* **447**, 465–468 (2004).
- 445 19. Fotiadis, D., Kanai, Y. & Palacín, M. Molecular Aspects of Medicine The SLC3 and SLC7
446 families of amino acid transporters. *Mol. Aspects Med.* **34**, 139–158 (2013).
- 447 20. Lin, T.-C. *et al.* Autophagy: Resetting glutamine-dependent metabolism and oxygen
448 consumption. *Autophagy* **8**, 1477–1493 (2012).
- 449 21. Coon, M. J. & Gurin, S. STUDIES ON THE CONVERSION OF RADIOACTIVE LEUCINE
450 TO ACETOACETATE. *J. Biol. Chem.* **180**, 1159–1167 (1949).
- 451 22. Xu, M. *et al.* Up-Regulation of LAT1 during Antiandrogen Therapy Contributes to
452 Progression in Prostate Cancer Cells. *J. Urol.* **195**, 1588–1597 (2016).
- 453 23. Verrey, F. *et al.* CATs and HATs: The SLC7 family of amino acid transporters. *Pflügers*
454 *Arch. Eur. J. Physiol.* **447**, 532–542 (2004).
- 455 24. Kaira, K. *et al.* L-Type amino acid transporter 1 (LAT1) expression in malignant pleural
456 mesothelioma. *Anticancer Res.* **31**, 4075–4082 (2011).
- 457 25. Isoda, A. *et al.* Expression of L-type amino acid transporter 1 (LAT1) as a prognostic and
458 therapeutic indicator in multiple myeloma. *Cancer Sci.* **105**, 1496–1502 (2014).
- 459 26. Kaira, K. *et al.* LAT1 expression is closely associated with hypoxic markers and mTOR in
460 resected non-small cell lung cancer. *Am. J. Transl. Res.* **3**, 468–478 (2011).
- 461 27. Shennan, D. B., Calvert, D. T., Travers, M. T., Kudo, Y. & Boyd, C. A. R. A study of L-
462 leucine, L-phenylalanine and L-alanine transport in the perfused rat mammary gland:
463 Possible involvement of LAT1 and LAT2. *Biochim. Biophys. Acta - Biomembr.* **1564**, 133–
464 139 (2002).
- 465 28. Poncet, N. *et al.* The catalytic subunit of the system L1 amino acid transporter (Slc7a5)
466 facilitates nutrient signalling in mouse skeletal muscle. *PLoS One* **9**, (2014).
- 467 29. Brunner, N. *et al.* Advances in Brief MCF7 / LCC2 : A 4-Hydroxytamoxifen Resistant
468 Human Breast Cancer Variant That Retains Sensitivity to the Steroidal Antiestrogen ICI
469 182 , 7801. 3229–3233 (1993).
- 470 30. Sweeney, E. E., McDaniel, R. E., Maximov, P. Y., Fan, P. & Jordan, V. C. Models and
471 mechanisms of acquired antihormone resistance in breast cancer: significant clinical
472 progress despite limitations. *Horm. Mol. Biol. Clin. Investig.* **9**, 143–163 (2012).
- 473 31. Clarke, R. *et al.* Molecular and pharmacological aspects of antiestrogen resistance. *J.*
474 *Steroid Biochem. Mol. Biol.* **76**, 71–84 (2001).
- 475 32. Feoktistova, M., Geserick, P. & Leverkus, M. Crystal violet assay for determining viability

of cultured cells. *Cold Spring Harb. Protoc.* **2016**, 343–346 (2016).

33. Sengupta, S., Biarnes, M. C., Clarke, R. & Jordan, V. C. Inhibition of BET proteins impairs estrogen-mediated growth and transcription in breast cancers by pausing RNA polymerase advancement. *Breast Cancer Res. Treat.* **150**, 265–278 (2015).
34. Sotiriou, C. *et al.* Gene Expression Profiling in Breast Cancer : Understanding the Molecular Basis of Histologic Grade To Improve Prognosis. **98**, (2006).
35. Loi, S. *et al.* Predicting prognosis using molecular profiling in estrogen receptor-positive breast cancer treated with tamoxifen. **12**, 1–12 (2008).
36. Loi, S. *et al.* JOURNAL OF CLINICAL ONCOLOGY Definition of Clinically Distinct Molecular Subtypes in Estrogen Receptor – Positive Breast Carcinomas Through Genomic Grade. **25**, (2019).
37. Pearce, D. A., Nirmal, A. J., Freeman, T. C. & Sims, A. H. Continuous Biomarker Assessment by Exhaustive Survival Analysis. *bioRxiv* (2018).
38. Shajahan-Haq, A. N. *et al.* EGR1 regulates cellular metabolism and survival in endocrine resistant breast cancer. *Oncotarget* **8**, 96865–96884 (2017).
39. Zhang, H. *et al.* Integrated proteogenomic characterization of human high grade serous ovarian cancer. **166**, 755–765 (2017).
40. Shennan, D. B., Thomson, J., Gow, I. F., Travers, M. T. & Barber, M. C. L -Leucine transport in human breast cancer cells (MCF-7 and MDA-MB-231): kinetics , regulation by estrogen and molecular identity of the transporter. **1664**, 206–216 (2004).
41. Consortium, T. E. P. An Integrated Encyclopedia of DNA Elements in the Human Genome. **489**, 57–74 (2012).
42. Davis, C. A. *et al.* The Encyclopedia of DNA elements (ENCODE): data portal update. **46**, 794–801 (2017).
43. Robinson, J. T. *et al.* Integrative genomics viewer. *Nat. Biotechnol.* **29**, 24 (2011).
44. Cormerais, Y. *et al.* Genetic disruption of the multifunctional CD98/LAT1 complex demonstrates the key role of essential amino acid transport in the control of mTORC1 and tumor growth. *Cancer Res.* **76**, 4481–4492 (2016).
45. Yothaisong, S. *et al.* Inhibition of L-type amino acid transporter 1 activity as a new therapeutic target for cholangiocarcinoma treatment. *Tumor Biol.* **39**, 101042831769454 (2017).
46. Schmidt, E. K., Clavarino, G., Ceppi, M. & Pierre, P. SUnSET, a nonradioactive method to monitor protein synthesis. *Nat. Methods* **6**, 275–277 (2009).
47. Cook, K. L. & Clarke, R. Estrogen receptor- α signaling and localization regulates autophagy and unfolded protein response activation in ER+ breast cancer. *Recept. Clin Investig* **1**, (2014).
48. Ohsumi, Y. Historical landmarks of autophagy research. *Cell Res.* **24**, 9–23 (2014).
49. Nosseri, C., Coppola, S. & Ghibelli, L. Possible Involvement of Poly(ADP-Ribosyl) Polymerase in Triggering Stress-Induced Apoptosis. *Exp. Cell Res.* **212**, 367–373 (1994).

50. Liang, Z. *et al.* Potential Biomarker of L-type Amino Acid Transporter 1 in Breast Cancer Progression. 93–102 (2011). doi:10.1007/s13139-010-0068-2
51. Cook, K. L., Shajahan, A. & Clarke, R. Autophagy and endocrine resistance in breast cancer. *Expert Rev Anticancer Ther* **11**, 1283–1294 (2011).
52. Martinez-Outschoorn, U. E., Peiris-Pagés, M., Pestell, R. G., Sotgia, F. & Lisanti, M. P. Cancer metabolism: A therapeutic perspective. *Nat. Rev. Clin. Oncol.* **14**, 11–31 (2017).
53. Devés, R., Angelo, S. & Chávez, P. N-ethylmaleimide discriminates between two lysine transport systems in human erythrocytes. *J. Physiol.* **468**, 753–66 (1993).
54. Shennan, D. B., Thomson, J., Barber, M. C. & Travers, M. T. Functional and molecular characteristics of system L in human breast cancer cells. *Biochim. Biophys. Acta - Biomembr.* **1611**, 81–90 (2003).
55. Müller, V., Jensen, E. V. & Knabbe, C. Partial antagonism between steroidal and nonsteroidal antiestrogens in human breast cancer cell lines. *Cancer Res.* **58**, 263–267 (1998).
56. Guan, B. J. *et al.* Translational control during endoplasmic reticulum stress beyond phosphorylation of the translation initiation factor eif2. *J. Biol. Chem.* **289**, 12593–12611 (2014).
57. Cook, K. L. *et al.* Endoplasmic Reticulum Stress Protein GRP78 Modulates Lipid Metabolism to Control Drug Sensitivity and Antitumor Immunity in Breast Cancer. *Cancer Res.* **76**, 5657 LP-5670 (2016).
58. Okana, N. *et al.* First-in-human phase I study of JPH203 in patients with advanced solid tumors. *J. Clin. Oncol.* **36**, 9–10 (2018).
59. Ueno, S., Kimura, T., Yamaga, T., Kawada, A. & Ochiai, T. Metformin enhances anti-tumor effect of L-type amino acid. *J. Pharmacol. Sci.* **1**, 1–8 (2016).
60. Sundaram, S. K. *et al.* Quantification of protein synthesis in the human brain using L-[1-¹¹C]-leucine PET: incorporation of factors for large neutral amino acids in plasma and for amino acids recycled from tissue. *J. Nucl. Med.* **47**, 1787–95 (2006).
61. Ansari, R. El *et al.* The amino acid transporter SLC7A5 confers a poor prognosis in the highly proliferative breast cancer subtypes and is a key therapeutic target in luminal B tumours. *Breast Cancer Res. 2018 201* **20**, 21 (2018).

FIGURE LEGENDS

Figure 1: LAT1 is estrogen regulated in endocrine therapy sensitive cell lines. A) LAT1 and CD98 are upregulated in endocrine therapy resistant cells (LCC9s) compared to sensitive cell lines (MCF7, LCC1s). B) This upregulation was observed in T47D:C42 and T47D:4HTs compared to parental T47D:A18s. C) ESR1 binding on the LAT1 gene. D) Increasing time of estrogen (1nM) increases LAT1 and CD98 mRNA in both MCF7 and LCC1 cells. E) MCF7 and F) LCC1 cells show increased protein levels of LAT1 with estrogen treatment.

Figure 2: LAT1 is not upregulated by estrogen in endocrine therapy resistant LCC9s. A) LAT1 nor CD98 are significantly changed at the mRNA level with estrogen treatment. B) Western blot analysis also showed no difference at the protein level. C) MCF7 and D) LCC9 cells look similar in immunofluorescent images as LAT1 and CD98 co-localize in both cell lines.

Figure 3: Endocrine therapies differentially change LAT1 expression in sensitive but not resistant cells. A) MCF7, B) LCC1, and C) LCC9 cell lines show differential LAT1 and CD98 protein or mRNA expression with endocrine therapy treatment for 24 hours. Endocrine therapy sensitive cells upregulate LAT1 and CD98 in response to estrogen and tamoxifen treatment.

Figure 4: LAT1 inhibition restricts MCF7 and LCC9 proliferation. A) MCF7 and B) LCC9 growth curves when treated with increasing doses of JPH203 for 3 and 6 days. C) siRNA targeting of LAT1 which is quantified in D) was more effective. E) Growth curve of siLAT1 cells showed a decrease in cell growth consistent for 3 or 6 days. Cell cycle analysis of F) MCF7 and G) LCC9 with JPH203 did not yield significant results, however H) siRNA knockdown of LAT1 in LCC9s reduced S phase. I) Western blot of puromycinylated proteins showed a reduction in global protein translation with LAT1 knock down after 72 hrs.

Figure 5: LAT1 Overexpression leads to proliferative advantage in MCF7 and LCC1s. LAT1 plasmid was transfected into cells with a GFP tag. A) MCF7 cells and B) LCC1 cells were sorted for GFP positivity confirmed LAT1 overexpression through western blot. C) microscopy image shows LAT1 overexpression in MCF7s. D) MCF7 cells were treated with puromycin to show increased global protein translation with LAT1 overexpression. Cell cycle analysis shows a trend increase of S phase in both E) MCF7 and F) LCC1 cells.

Figure 6: Autophagy initiates but does not complete with LAT1 inhibition. A) markers for autophagy and the unfolded protein response show autophagic flux. B) knockdown of GRP78 shows an increase of LAT1 protein after 72 hours. C) The mRNA levels of LAT1 increase with GRP78 knockdown (one replicate is stronger than the other).

Figure 7: Clinical data sets confirm increased LAT1 expression correlates with poor disease-free survival.

Table 1: List of significantly differentially regulated genes in LCC9s compared to LCC1s at mRNA analysis and compared with clinical data sets. Three clinical data sets are used: Edinburgh (GSE46222), LoiPlus2 (GSE9195), and Sotiriou (GSE299). For some SLCs multiple probesets exist. For mRNA analysis, p value, FDR, and fold change (FC) exist with FC indicated with positive (red) numbers meaning upregulation and negative (green) numbers meaning downregulation in the LCC9 compared to the LCC1 cells. For the GSE data sets, the direction of high or low expression of the given SLC is indicated for poor prognosis with the p value. Edinburgh and LoiPlus2 utilized the affymetrix HG-U133plus2 chip set while Sotiriou used affymetrix HG-U133A chip set resulting in some genes not being included (marked yellow as invalid gene symbol). Non-significant KM data is marked in red as NS.

Table 2: List of significantly upregulated (1.5 fold or more) solute carriers in LCC9 cells compared to LCC1 cells in mRNA, TMT, and SILAC analysis. Red text indicates upregulation in all three data sets.

Supplemental Data to Include:

Supplemental Figure 1: ESR1 protein binds to an early portion of the LAT1 gene in MCF7 cells as shown by ChIA-PET.

Supplemental Figure 2: GREB1 is classically expressed in response to endocrine therapy treatment in MCF7 but not LCC9s. A) GREB1 mRNA expression increases with estrogen treatment. B) GREB1 mRNA does not change in response to endocrine therapy treatment showing classical estrogen regulation which is lost in C) LCC9 cells.

Supplemental Figure 3: Endocrine therapy treatment modulates LAT1 expression in A) endocrine therapy sensitive T47D:A18s but not endocrine therapy resistant B) T47D:C42s nor C) T47D:4HTs.

Supplemental Figure 4: Depleting essential amino acids in the media enhances growth arrest by JPH203 in both LCC9s and C42s. A) LCC9s or B) T47D:C42s were cultured in essential amino acid deplete media and treated with indicated concentrations of JPH203 resulting in increased efficacy. C) LCC9 and D) T47D:C42 cells had an increase in Sub G1 when analyzed by flow cytometry and E-F) both showed a decrease in S phase.

LAT1 Paper Figures

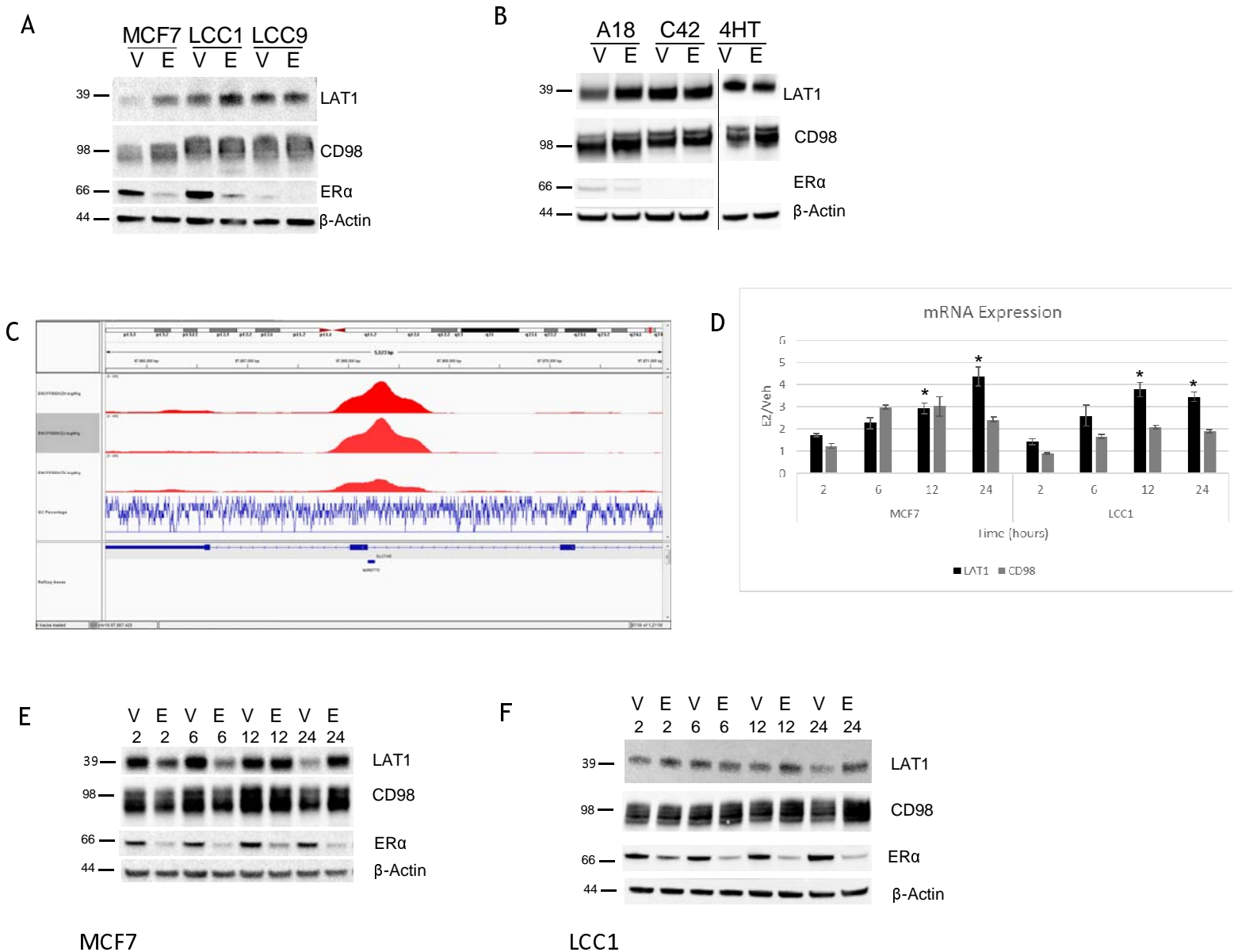


Figure 1.

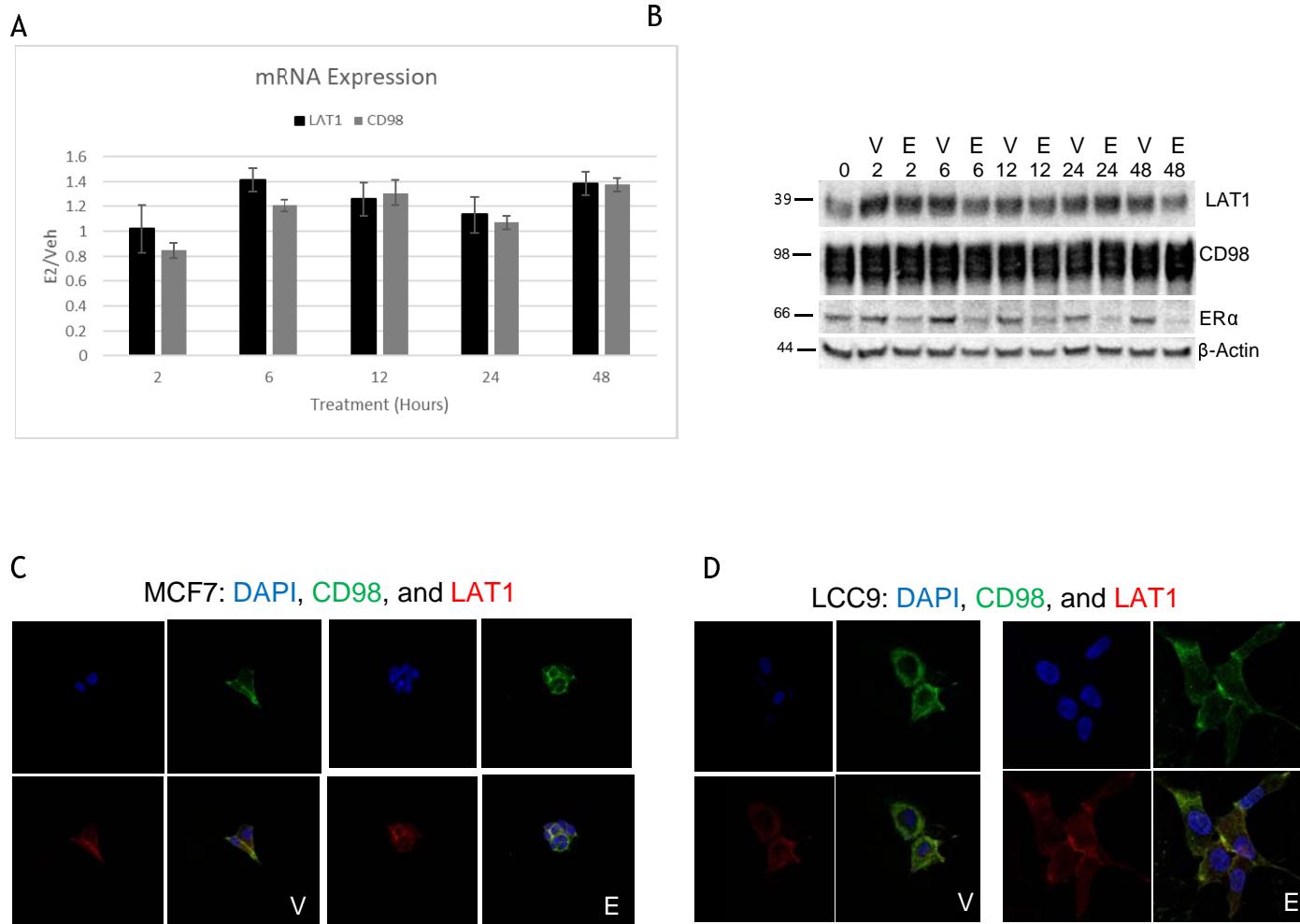


Figure 2

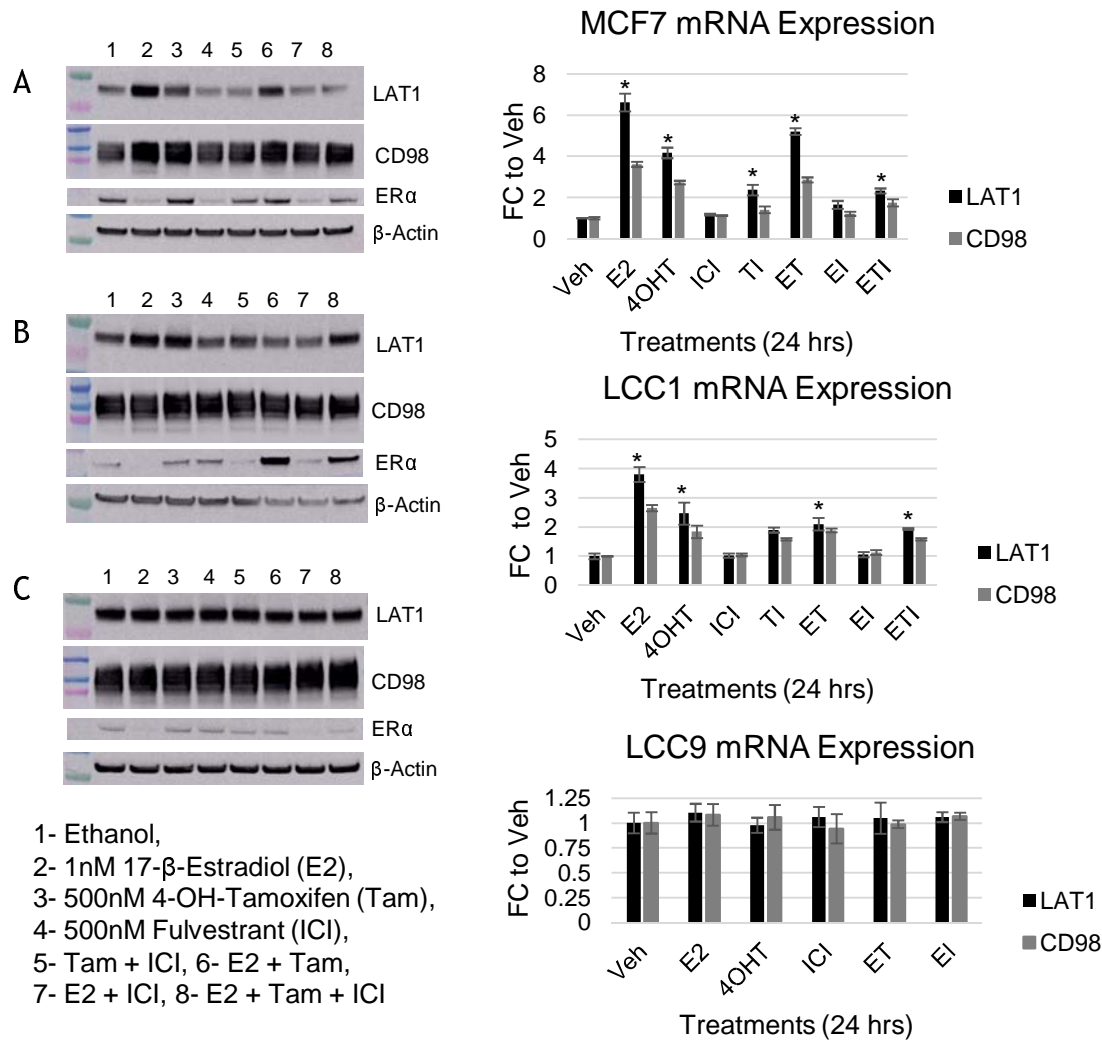


Figure 3

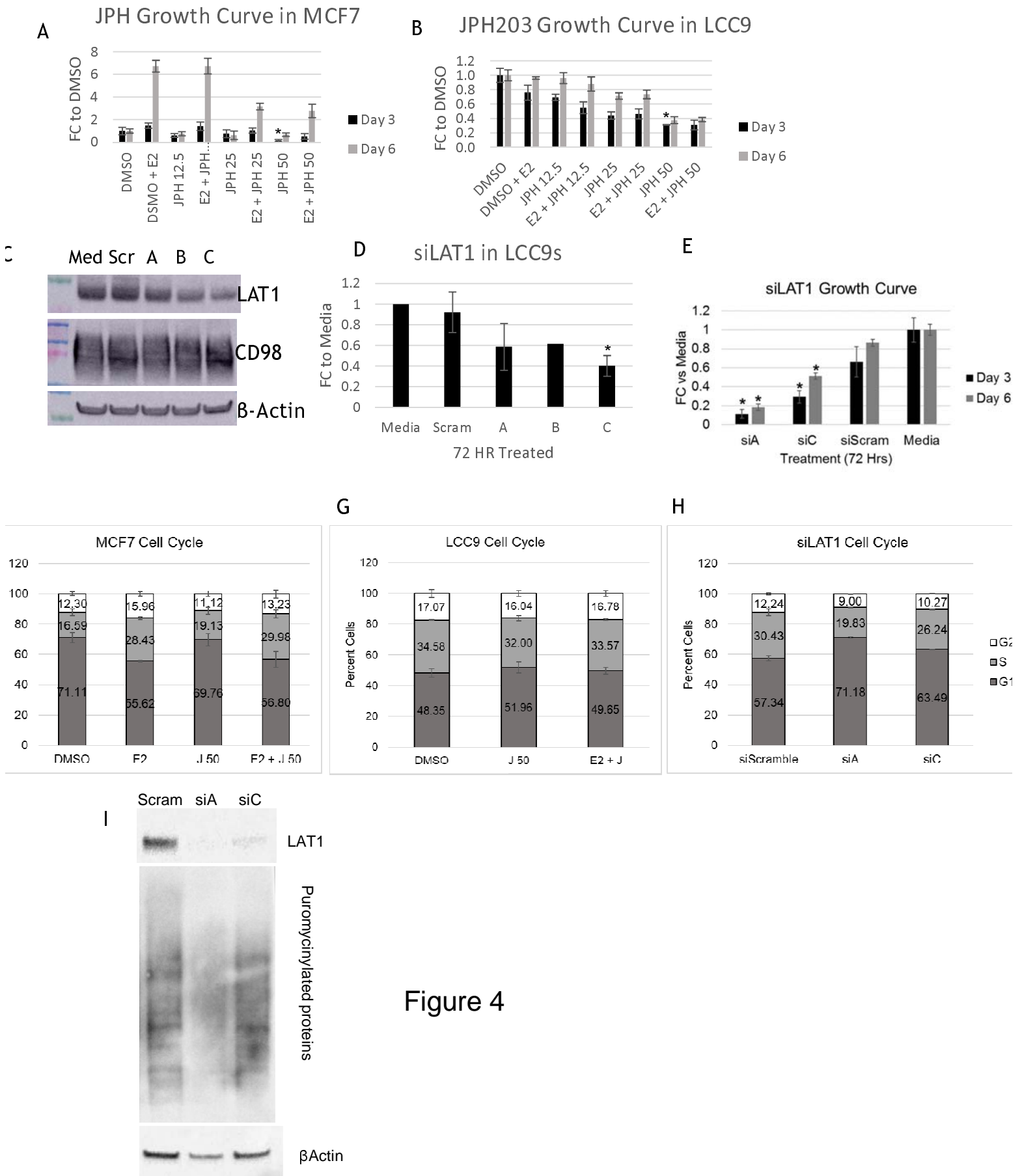
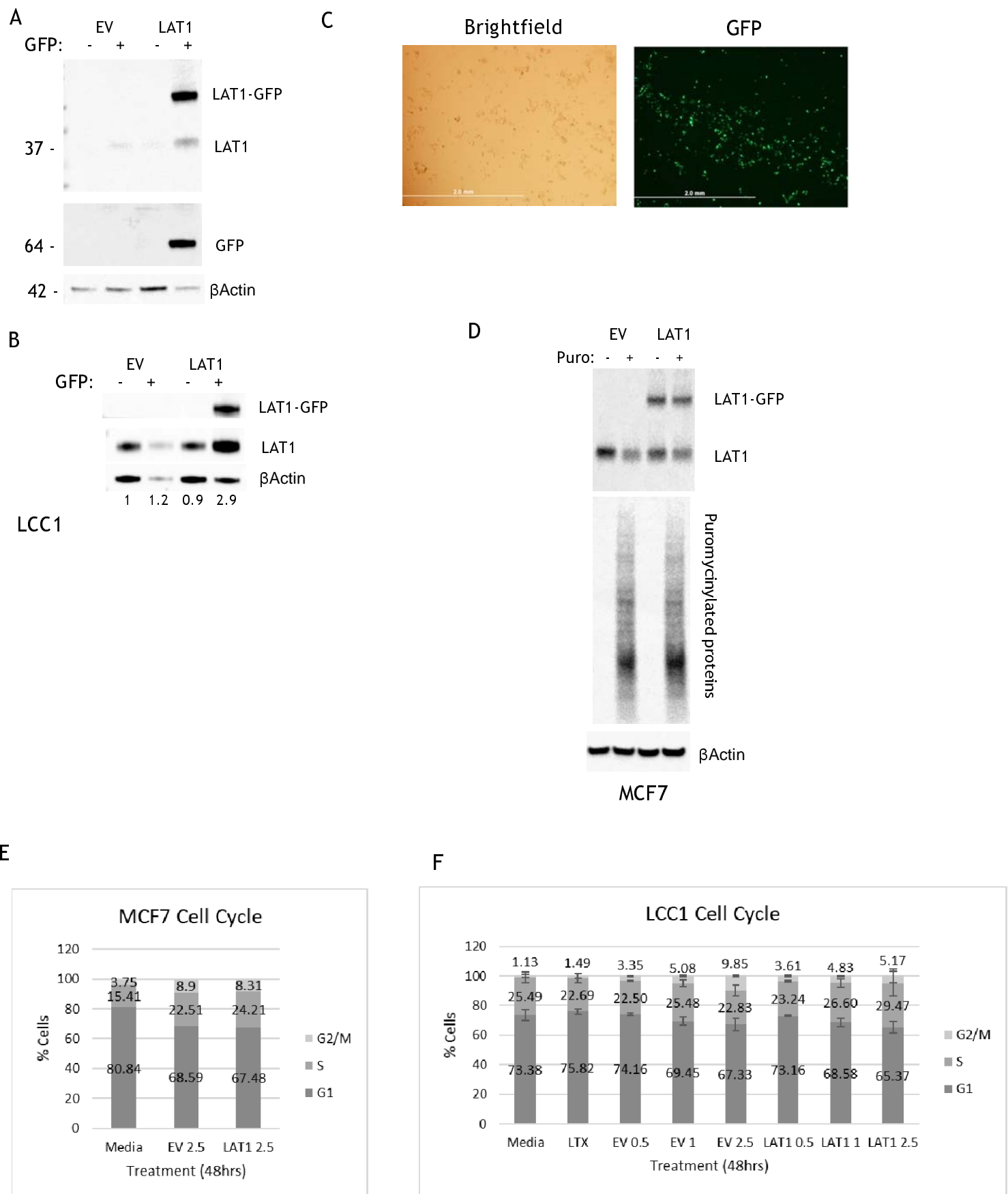


Figure 4

Figure 5



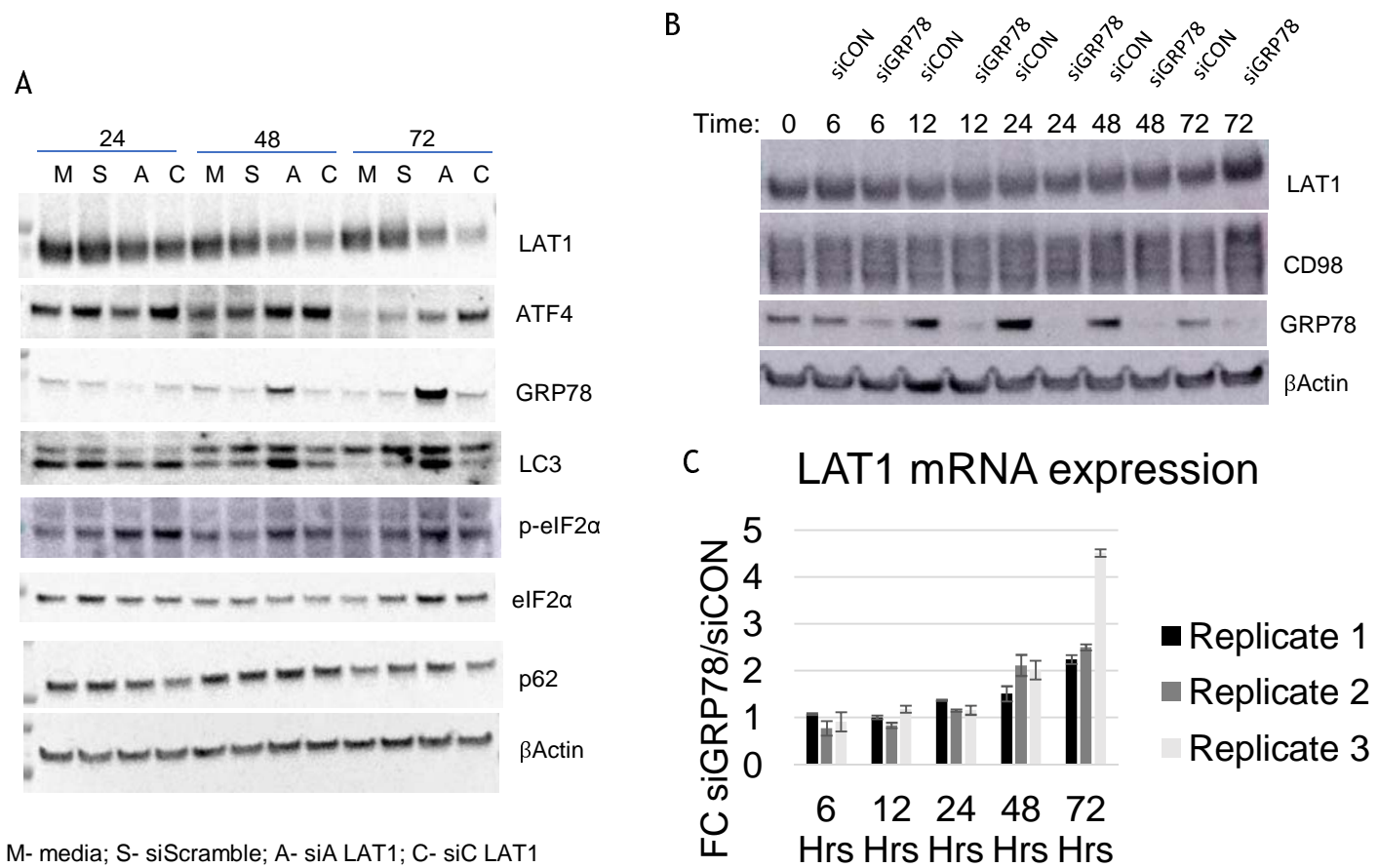
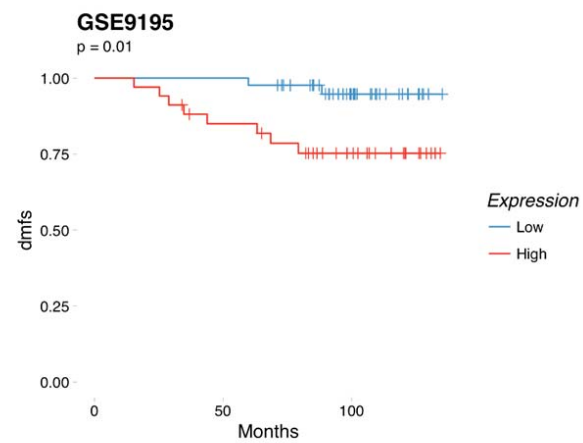
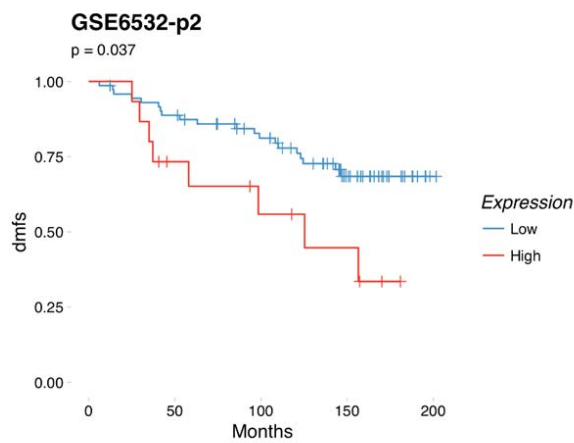
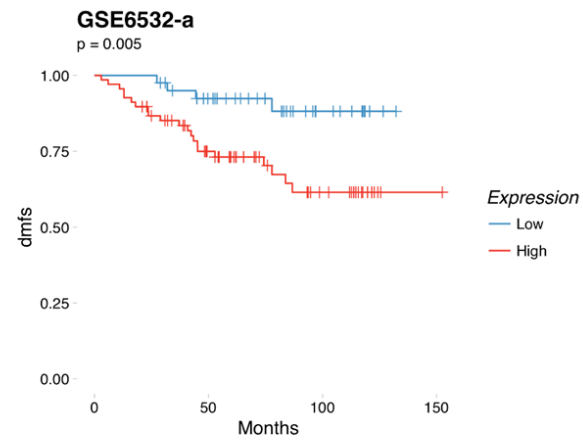
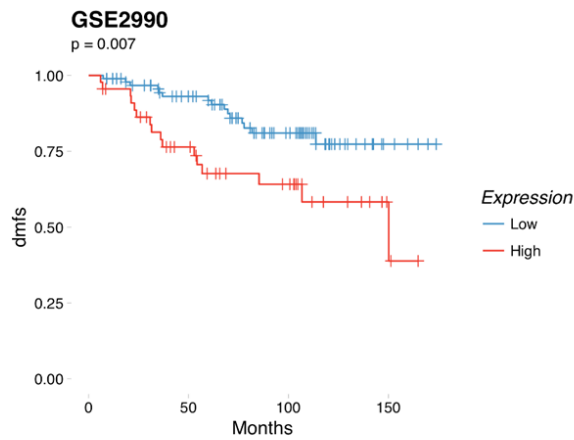


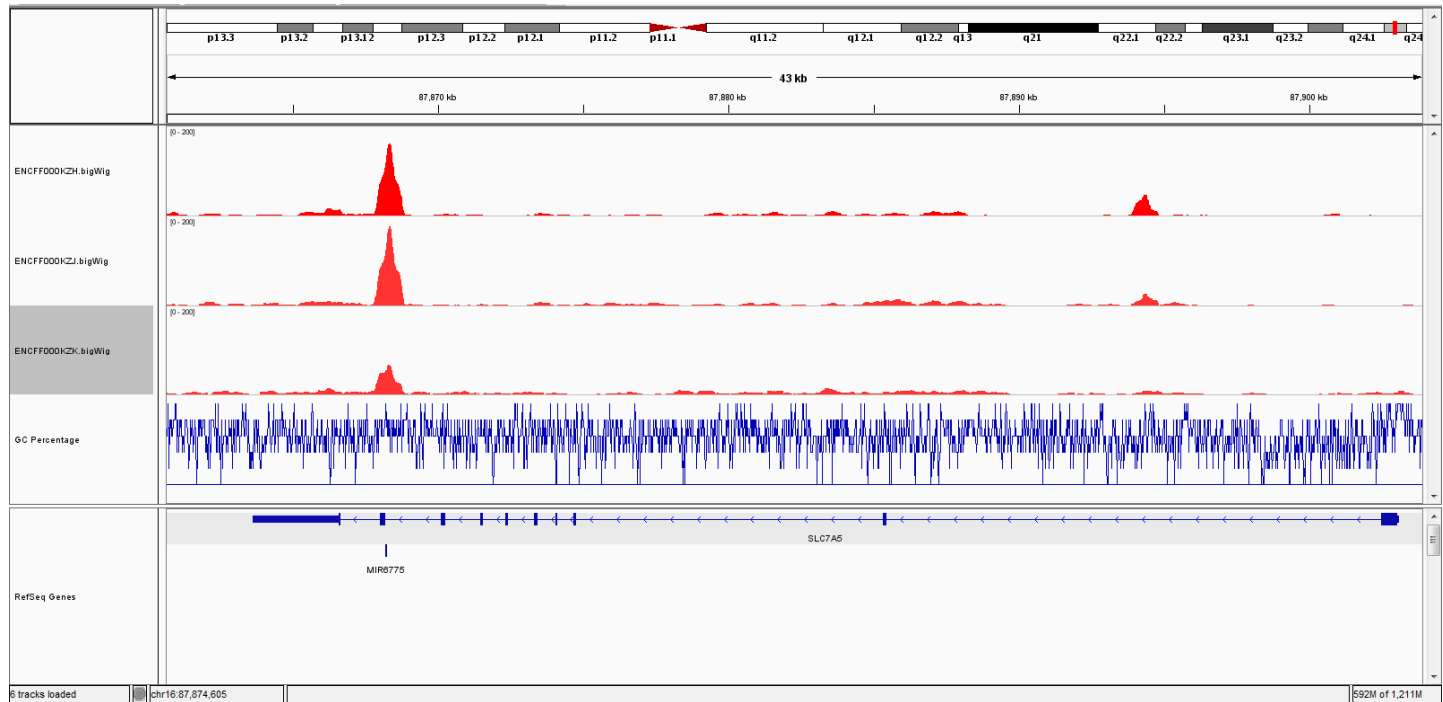
Figure 6

Figure 7

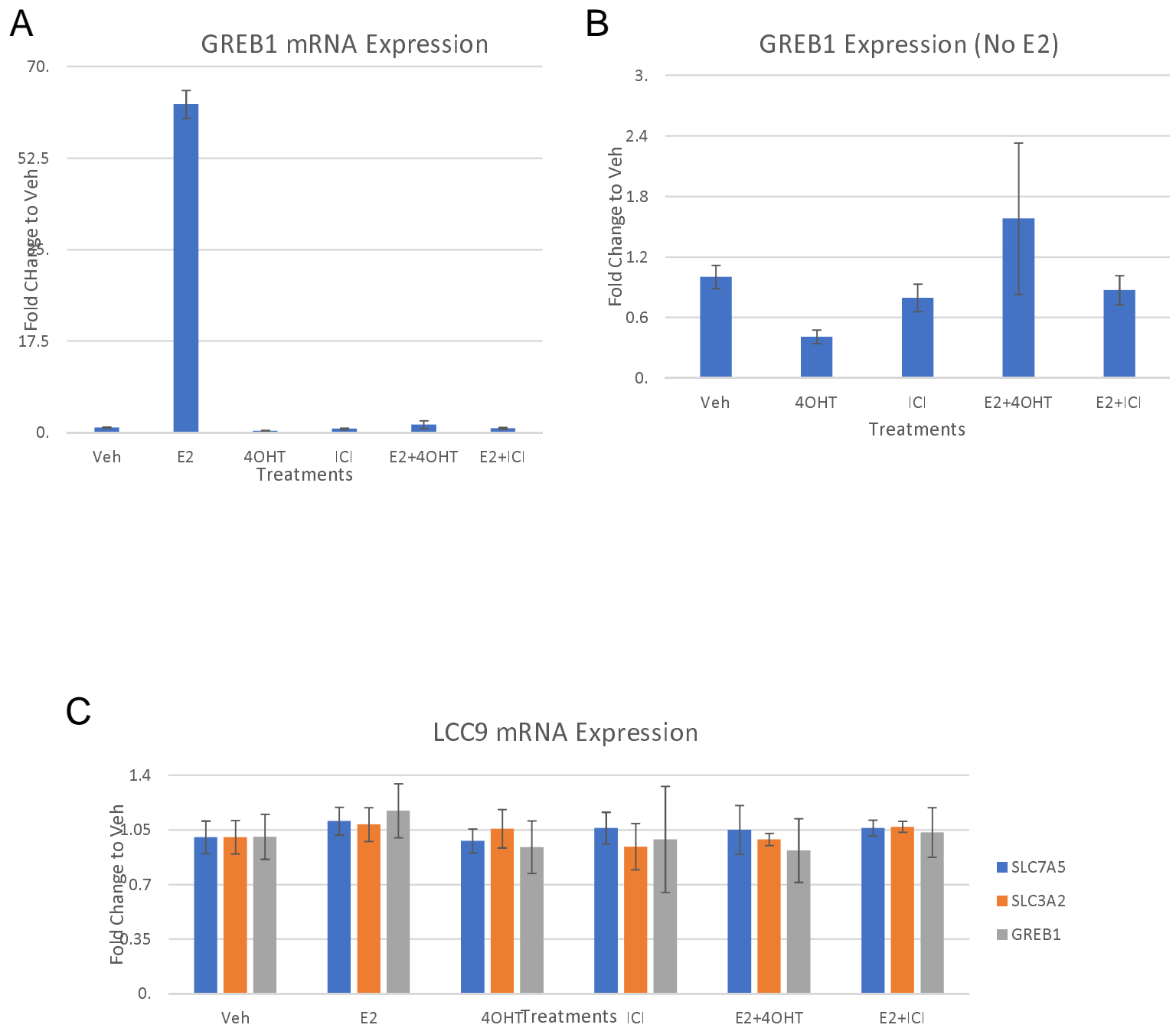
SLC7A5



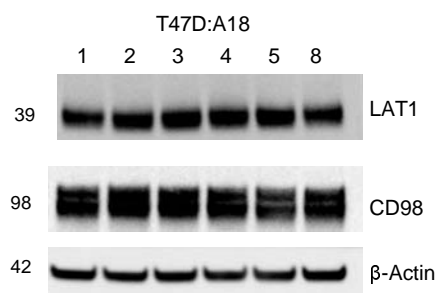
Supplemental Figure 1



Supplemental Figure 2

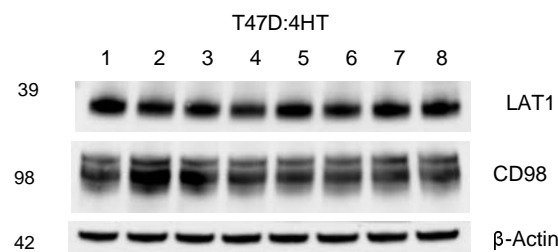
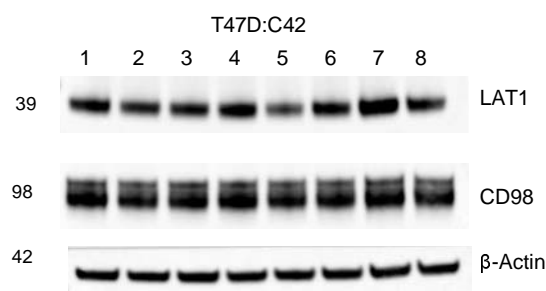


A



Supplemental Figure 3

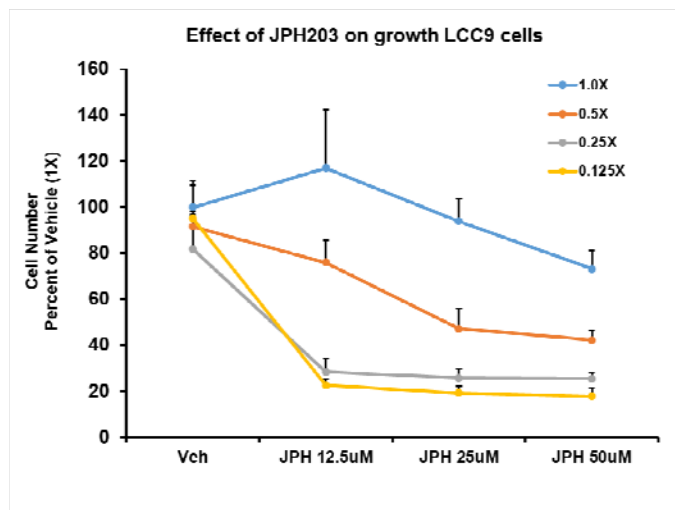
3



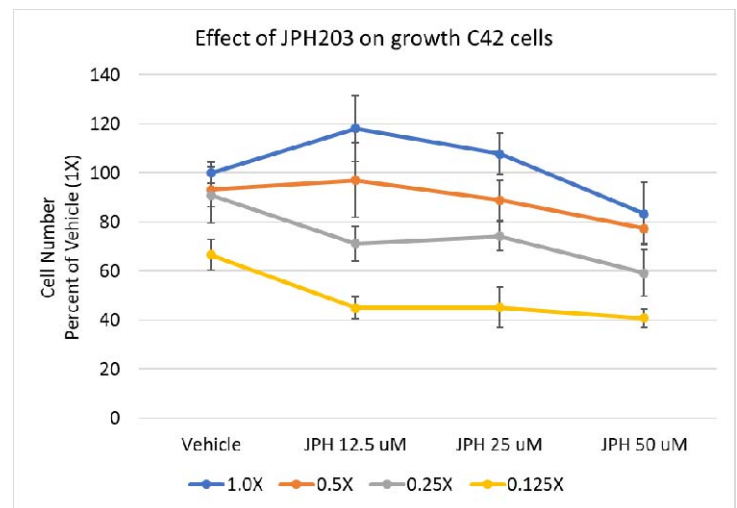
- 1- Ethanol,
- 2- 1nM 17-β-Estradiol (E2),
- 3- 500nM 4-OH-Tamoxifen (Tam),
- 4- 500nM Fulvestrant (ICI),
- 5- E2 + Tam, 6- E2 + ICI,
- 7- Tam + ICI, 8- E2 + Tam + ICI

Supplemental Figure 4

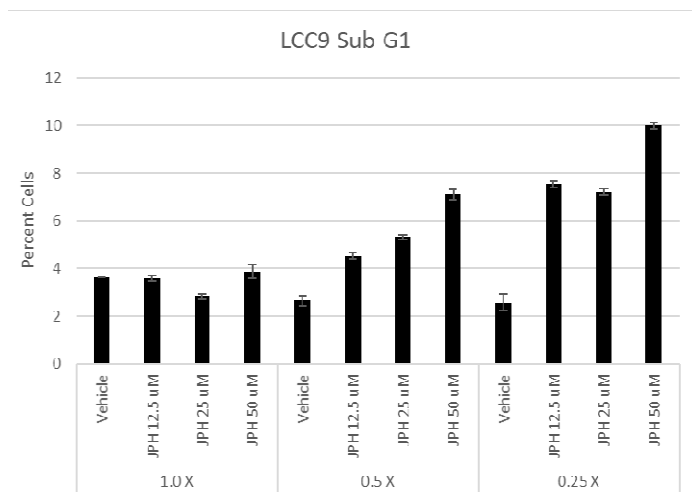
A



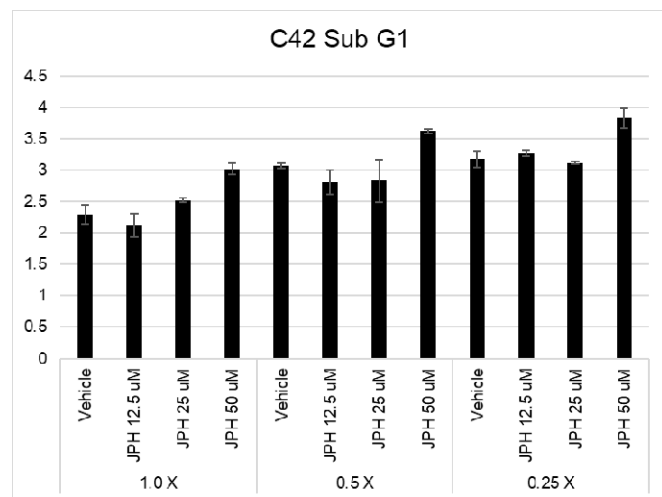
B



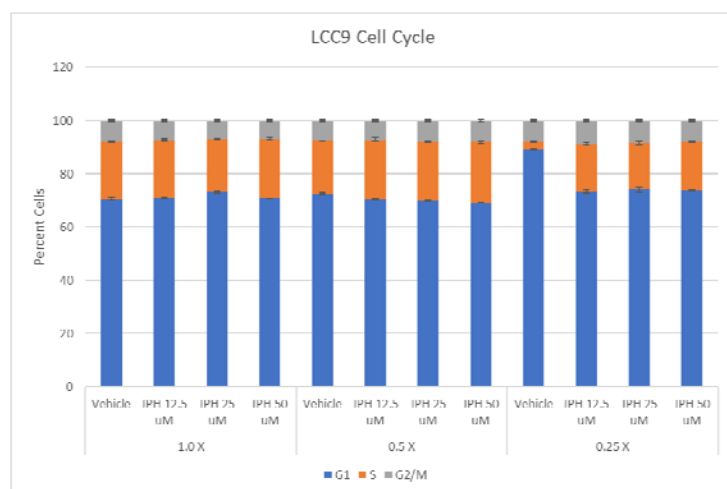
C



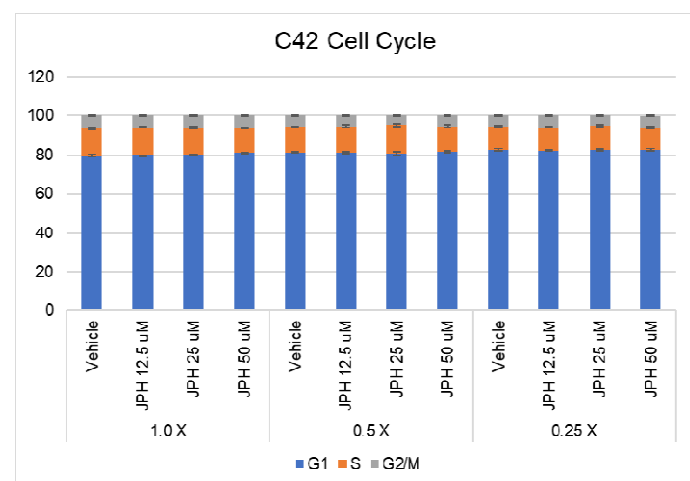
D



E



F



gene_symbol	probeset_id	p.value	fdr	FC	Edinburgh_Lite (GSE46222)	LoiPlus2_Lite (GSE9195)	Sotiriou_Lite (GSE2990)
CENPA /// SLC35F6	204962_s_at	5.17E-05	0.004569	1.617387	High 7.875, p=0.0034	High 5.285, p=0.029	High 5.965, p=0.05
LOC100271836 /// LOC101010	208118_x_at	0.003438694	0.026045	-1.11751	High 8.095, p=0.011	NS	NS
LOC653562 /// SLC6A10P	215812_s_at	0.002117504	0.020492	1.710179	High 6.935, p=0.049	NS	NS
MIR4647 /// SLC35B2	224716_at	0.004229602	0.028951	1.322054	NS	High 7.4, p=0.033	Invalid Gene Symbol
SLC10A7	235143_at	0.002596109	0.022627	1.195727	High 8.495, p=0.029	NS	Invalid Gene Symbol
SLC11A2	203124_s_at	0.036832926	0.099652	1.076462	NS	NS	NS
SLC12A2	204404_at	0.000770582	0.012463	-3.45577	NS	NS	Low 7.645, p=0.037
SLC12A2	225835_at	0.001851156	0.019123	-3.03612	NS	NS	Invalid Gene Symbol
SLC12A7	218066_at	0.010435669	0.047084	-1.4232	Low 10.3, p=0.044	NS	NS
SLC15A4	225057_at	0.00728947	0.038527	-1.14875	NS	NS	Invalid Gene Symbol
SLC16A14	238029_s_at	0.000584612	0.011019	-4.98235	Low 7.14, p=0.026	Low 5.26, p=0.028	Invalid Gene Symbol
SLC16A4	205234_at	0.004432008	0.029757	2.596924	Low 6.665, p=0.026	NS	Invalid Gene Symbol
SLC16A5	206600_s_at	0.000129478	0.006101	1.580061	Low 8.485, p=0.043	Low 4.975, p=0.039	NS
SLC16A5	213590_at	0.007189441	0.038257	1.339344	Low 6.09, p=0.046	Low 4.055, p=0.041	NS
SLC16A5	206599_at	0.01573788	0.059207	1.486868	Low 5.305, p=0.033	NS	High 6.335, p=0.046
SLC16A6	207038_at	0.009688796	0.045121	-1.15262	High 7.9, p=0.043	Low 3.475, p=0.047	Low 4.49, p=0.046
SLC16A6	230748_at	0.001325825	0.016146	-1.30478	High 11.03, p=0.047	Low 6.6, p=0.041	Invalid Gene Symbol
SLC17A5	223441_at	0.028052973	0.083939	1.209584	NS	Low 7.47, p=0.021	Invalid Gene Symbol
SLC18B1	226301_at	0.001711399	0.018286	2.445649	NS	NS	Invalid Gene Symbol
SLC19A1	1555953_at	0.015246247	0.058167	1.18935	High 5.555, p=0.0023	High 2.785, p=0.012	Invalid Gene Symbol
SLC19A1	211576_s_at	0.029848244	0.087349	1.06119	High 8.465, p=0.036	NS	NS
SLC19A1	209776_s_at	0.018217152	0.064946	1.250898	NS	High 2.685, p=0.039	NS
SLC19A1	1555952_at	0.002808328	0.023522	1.139643	NS	High 4.035, p=0.018	Invalid Gene Symbol
SLC1A2	225491_at	0.000982138	0.013991	2.649049	Low 6.485, p=0.033	High 6.15, p=0.041	Invalid Gene Symbol
SLC1A2	208389_s_at	0.023254599	0.075263	1.427787	NS	High 3.37, p=0.019	NS
SLC1A4	212811_x_at	0.006485715	0.036339	1.159583	NS	NS	NS
SLC1A4	212810_s_at	0.037848284	0.101473	1.209032	NS	NS	NS
SLC1A4	209610_s_at	0.02974529	0.087148	1.091085	NS	NS	NS
SLC20A1	230494_at	0.000450945	0.009864	-2.25753	NS	NS	Invalid Gene Symbol
SLC22A17	218675_at	0.013646101	0.054535	-1.43223	Low 7.01, p=0.048	Low 4.935, p=0.0082	NS
SLC22A23	223194_s_at	0.048866263	0.119523	-1.17048	High 9.99, p=0.047	Low 6.745, p=0.049	Invalid Gene Symbol
SLC22A25	1561093_at	0.048995969	0.119698	1.162918	NS	High 4.36, p=0.041	Invalid Gene Symbol
SLC22A4	205896_at	0.000634784	0.0114	-1.63342	NS	NS	Low 6.105, p=0.044
SLC22A5	205074_at	0.004559216	0.030155	-1.2658	NS	High 7.185, p=0.04	Low 6.75, p=0.04
SLC24A3	57588_at	8.43E-05	0.005376	-8.34833	NS	NS	NS
SLC24A3	219090_at	0.000931476	0.013575	-14.2258	NS	NS	NS
SLC25A1	210010_s_at	0.005611666	0.033637	-1.2367	High 7.56, p=0.045	High 6.485, p=0.043	High 8.445, p=0.046
SLC25A14	211855_s_at	0.013340296	0.053763	1.108155	NS	High 5.77, p=0.044	NS
SLC25A19	223222_at	0.042825061	0.109717	1.152791	High 8.095, p=0.037	High 5.62, p=0.018	Invalid Gene Symbol
SLC25A21	220474_at	0.05569601	0.129773	-1.82493	Low 5.215, p=0.0041	Low 1.88, p=0.027	NS
SLC25A23	226010_at	0.010451344	0.047101	-1.32443	Low 6.95, p=0.046	High 5.98, p=0.027	Invalid Gene Symbol
SLC25A25	225212_at	0.015776261	0.059295	1.325573	NS	High 6.125, p=0.036	Invalid Gene Symbol
SLC25A29	225305_at	0.021826985	0.072434	-1.17237	NS	Low 6.975, p=0.043	Invalid Gene Symbol
SLC25A29	225306_s_at	0.025837651	0.080016	-1.12338	NS	NS	Invalid Gene Symbol
SLC25A3	200030_s_at	0.000104836	0.005791	1.154469	NS	NS	NS
SLC25A30	226782_at	0.004771092	0.030832	-1.73303	NS	High 6.145, p=0.043	Invalid Gene Symbol
SLC25A32	221020_s_at	0.043678816	0.111235	1.184943	High 9.66, p=0.019	High 7.73, p=0.04	High 7.7, p=0.03
SLC25A33	223296_at	0.000668449	0.011646	1.398479	High 9.445, p=0.044	NS	Invalid Gene Symbol
SLC25A36	201917_s_at	0.000317131	0.00844	-1.43304	High 11.21, p=0.043	NS	High p=0.046
SLC25A36	201919_at	0.001146015	0.015037	-1.41156	Low 10.64, p=0.039	NS	NS
SLC25A36	201918_at	0.001805146	0.018832	-1.60159	NS	NS	NS
SLC25A38	217961_at	0.005111948	0.032069	1.247872	NS	NS	Low 5.97, p=0.021
SLC25A4	202825_at	0.040584996	0.106292	1.091067	NS	High 6.78, p=0.027	NS
SLC25A40	227012_at	0.026956423	0.081997	-1.37686	Low 8.68, p=0.035	High 7.43, p=0.039	Invalid Gene Symbol
SLC25A40	205716_at	0.005888052	0.034482	-1.404	NS	High 4.74, p=0.024	Low 6.335, p=0.036
SLC25A44	32091_at	0.0109647	0.048283	-1.25072	NS	Low 7.95, p=0.035	NS
SLC25A44	212683_at	0.004170427	0.028784	-1.19602	NS	NS	NS
SLC25A5	200657_at	0.006823705	0.037259	1.072196	NS	High 10.32, p=0.05	NS
SLC25A6	212085_at	0.043209477	0.110363	-1.07639	High 11.52, p=0.039	NS	Low 9.82, p=0.027
SLC26A2	224959_at	5.82E-05	0.004782	3.173992	High 10.6, p=0.049	Low 7.18, p=0.045	Invalid Gene Symbol
SLC26A2	205097_at	9.20E-05	0.005514	3.180374	Low 8.135, p=0.023	NS	NS
SLC26A2	224963_at	0.000914532	0.013466	3.060895	NS	Low 4.82, p=0.035	Invalid Gene Symbol
SLC27A2	205769_at	2.29E-05	0.003521	-1.94835	NS	NS	NS
SLC27A2	205768_s_at	0.000260504	0.007732	-2.03837	NS	NS	NS
SLC27A3	222217_s_at	0.002155163	0.020659	-1.81458	High 8.575, 0.012	High 5.69, p=0.043	High 8.285, p=0.028
SLC27A5	219733_s_at	0.004606651	0.030236	1.218387	NS	NS	NS
SLC27A6	219932_at	0.001001026	0.014165	-2.22383	NS	Low 2.295, p=0.0037	NS
SLC29A1	201801_s_at	0.001034882	0.014349	1.432326	NS	NS	NS
SLC29A3	219344_at	0.000222447	0.007235	2.163405	NS	NS	High 9.015, p=0.044
SLC2A1	201250_s_at	0.005870616	0.034431	1.605866	Low 9.185, p=0.039	High 5.69, p=0.0038	NS
SLC2A10	221024_s_at	0.000843918	0.012926	-2.06319	NS	High 8.605, p=0.047	NS
SLC2A11	1558540_s_at	0.026304402	0.080811	1.192472	High 6.325, p=0.0023	NS	Invalid Gene Symbol
SLC2A4RG	1555500_s_at	0.024777066	0.078096	-1.23669	High 7.215, p=0.024	High 4.64, p=0.043	Invalid Gene Symbol
SLC2A4RG	218494_s_at	0.0057673	0.034133	-1.42244	NS	NS	High 9.715, p=0.048
SLC2A8	218985_at	0.038248928	0.102103	1.101812	High 7.48, p=0.023	High 5.74, p=0.039	NS
SLC30A1	228181_at	0.023485584	0.075686	1.338999	Low 5.905, p=0.045	Low 5.285, p=0.036	Invalid Gene Symbol
SLC30A5	220181_x_at	0.041139669	0.107193	1.26106	High 7.215, p=0.049	High 4.485, p=0.0015	NS
SLC30A7	226601_at	0.011948637	0.050518	1.369935	Low 9.655, p=0.017	Low 7.655, p=0.036	Invalid Gene Symbol
SLC30A9	202614_at	0.031587148	0.090433	-1.20326	Low 8.975, p=0.024	Low 7.915, p=0.048	NS
SLC31A1	203971_at	0.025861965	0.080061	1.223299	High 9.905, p=0.017	Low 6.32, p=0.048	NS
SLC31A2	204204_at	0.024571229	0.077709	1.387525	Low 7.06, p=0.04	NS	Low 7.97, p=0.041
SLC35A1	203306_s_at	0.013328677	0.053744	-1.2577	NS	NS	NS
SLC35A2	209326_at	0.013163845	0.053306	1.246032	High 9.875, p=0.024	NS	NS
SLC35A3	206770_s_at	0.011853567	0.05039	-1.24747	Low 8.705, p=0.035	NS	NS
SLC35B1	202433_at	0.003544071	0.026416	1.164279	NS	High 8.04, p=0.031	High 9.62, p=0.046
SLC35B4	225881_at	0.001171479	0.015262	1.218192	Low 7.68, p=0.02	NS	Invalid Gene Symbol
SLC35B4	225882_at	0.008234727	0.040965	1.201619	NS	NS	Invalid Gene Symbol
SLC35C1	222647_at	0.00211897	0.020497	1.145549	High 7.195, p=0.042	NS	Invalid Gene Symbol
SLC35C2	219447_s_at	0.021453508	0.071672	1.204109	NS	NS	NS
SLC35C2	225037_at	0.023679483	0.076069	1.198898	NS	NS	Invalid Gene Symbol
SLC35D2	213083_at	0.030153189	0.087842	1.110658	High 10.24, p=0.038	NS	Low 6.495, p=0.036
SLC35E2 /// SLC35E2B	217122_s_at	0.026061191	0.080359	-1.19451	High 12.21, p=0.034	Low 9.205, p=0.0031	Low 10.24, p=0.01
SLC35E3	218988_at	0.024612587	0.077808	1.174233	NS	High 7.35, p=0.048	NS
SLC35F1	228060_at	0.001632989	0.017866	-1.30187	NS	NS	Invalid Gene Symbol
SLC35F5	225872_at	0.033125176	0.093274	-1.23779	NS	NS	Invalid Gene Symbol
SLC36A1	213119_at	0.007931184	0.040282	-1.11336	NS	High 6.46, p=0.049	NS
SLC36A4	234978_at	0.028179342	0.084239	1.450574	NS	NS	Invalid Gene Symbol
SLC37A1	218928_s_at	0.00061643	0.011234	-1.25231	NS	NS	Low 5.055, p=0.05
SLC37A3	223304_at	0.026500761	0.081169	1.182426	NS	Low 6.925, p=0.048	Invalid Gene Symbol
SLC38A1	224580_at	0.002017701	0.01997	-1.94741	Low 7.015, p=0.047	NS	Invalid Gene Symbol
SLC38A1	218237_s_at	0.000209885	0.007116	-1.87755	NS	NS	Low 9.045, p=0.042
SLC38A1	224579_at	0.000268862	0.007831	-1.73485	NS	NS	Invalid Gene Symbol
SLC38A10	212890_at	0.000621855	0.011242	-1.45394	High 10.18, p=0.045	Low 7.025, p=0.031	Low 9.295, p=0.047
SLC38A7	228951_at	0.038926448	0.10337	1.710319	High 7.035, p=0.049	High 5.12, p=0.037	Invalid Gene Symbol
SLC38A7	56821_at	0.012910532	0.052663	1.229117	High 7.075, p=0.045	NS	NS
SLC38A7	218727_at	0.03928612	0.104007	1.37501	NS	NS	NS
SLC38A9	235241_at	0.03464121	0.096007	-1.07814	NS	Low 5.995, p=0.039	Invalid Gene Symbol
SLC39A14	212110_at	0.037494522	0.100836	1.125249	Low 9.605, p=0.028	Low 7.7325, p=0.031	Low 8.345, p=0.048
SLC39A3	223917_s_at	0.000491043	0.010332	1.232901	NS	NS	Invalid Gene Symbol
SLC39A6	202088_at	0.002902268	0.023924	1.39137	Low 13.02, p=0.039	NS	NS
SLC39A6	1555460_a_at	0.007209525	0.038286	1.771934	Low 7.26, p=0.034	NS	Invalid Gene Symbol
SLC39A6	1556551_s_at	0.02373752	0.076153	1.595159	NS	High 9.155, p=0.036	Invalid Gene Symbol
SLC39A6	202089_s_at	0.002932021	0.024003	1.680305	NS	NS	NS
SLC39A8	209267_s_at	8.35E-05	0.005357	-2.39285	Low 8.27, p=0.043	Low 6.155, p=0.043	NS
SLC39A8	219869_s_at	0.000115796	0.005842	-1.83556	NS	Low 3.955, p=0.048	NS
SLC3A2	200924_s_at	0.000306255	0.008263	2.119842	High 9.335, p=0.047	NS	High 8.93, p=0.047
SLC41A1	225570_at	0.025066312	0.078627	1.22062	High 8.46, p=0.036	NS	Invalid Gene Symbol
SLC41A2	223798_at	0.011912105	0.050484	-1.37303	High 6.825, p=0.039	Low 3.955, p=0.04	Invalid Gene Symbol
SLC41A2	235299_at	0.025917089					

TMT	SILAC	mRNA
SLC1A4		SLC1A4
SLC1A5		
SLC2A1	SLC2A1	SLC2A1
SLC3A2	SLC3A2	SLC3A2
SLC4A1AP		
SLC4A2		
SLC4A7		
SLC5A6		
SLC6A6		
		SLC6A8
SLC6A14		SLC6A14
SLC7A1		
SLC7A2		
SLC7A5	SLC7A5	SLC7A5
SLC7A6		
SLC7A6OS		SLC7A6OS
		SLC7A11
SLC9A1		
SLC9A3R1	SLC9A3R1	
SLC9A3R2		
SLC9A3R2		
SLC9A7		SLC9A7
SLC9A8		
SLC11A2		
SLC12A2		SLC12A2
SLC12A6		
SLC12A7		
SLC12A9		
SLC16A1		
SLC16A3		
SLC19A2		
SLC22A18		
SLC25A1		
SLC25A3	SLC25A3	
SLC25A4	SLC25A4	
SLC25A5		
SLC25A6	SLC25A6	
SLC25A10	SLC25A10	
SLC25A11	SLC25A11	
SLC25A12		
SLC25A13	SLC25A13	
SLC25A15		
SLC25A17		
SLC25A19		SLC25A19
SLC25A20		
SLC25A22		
		SLC25A23
SLC25A24		
SLC25A25		
SLC25A29		
		SLC25A30
		SLC25A33
SLC25A32		
SLC25A36		SLC25A36
SLC25A40		
SLC25A44		SLC25A44
SLC25A46		
		SLC26A2
SLC27A1		
SLC27A2		SLC27A2
SLC27A3		SLC27A3
SLC27A4		
<small>bioRxiv preprint doi: https://doi.org/10.1101/555342; this version posted February 21, 2019. The copyright holder for this preprint (which was not certified by peer review) is the author/funder, who has granted bioRxiv a license to display the preprint in perpetuity. It is made available under aCC-BY-NC-ND 4.0 International license.</small>		
		SLC27A6
SLC29A1		
SLC30A5		SLC30A5
SLC30A6		
SLC30A7		SLC30A7
SLC30A9		
SLC33A1		
SLC35A1		
SLC35B2		MIR4647 /// SLC35B2
SLC35C2		
SLC35E1		
SLC35F6		CENPA /// SLC35F6
SLC37A1		SLC37A1
SLC37A4		
SLC38A1		SLC38A1
SLC38A2		
SLC38A10		
SLC39A6		SLC39A6
SLC39A7		
		SLC39A8
SLC39A10		
SLC39A11		
SLC39A14		
		SLC41A2
SLC41A3		
SLC44A1		
SLC44A2		
SLC50A1		